Annual Reviews in Control 000 (2015) 1–15

Contents lists available at ScienceDirect

Annual Reviews in Control

journal homepage: www.elsevier.com/locate/arcontrol

Full length article

Observability analysis of 3D AUV trimming trajectories in the presence of ocean currents using range and depth measurements☆,☆☆

N. Crasta[a,*], M. Bayat[a,b], António Pedro Aguiar[c], António M. Pascoal[a]

[a] Laboratory of Robotics and Systems in Engineering and Science (LARSyS), IST/University of Lisbon, Av. Rovisco Pais, 1, 1049-001 Lisbon, Portugal
[b] Biorobotics Laboratory, Ecole Polytechnique Fédérale de Lausanne, Station 14, CH-1015 Lausanne, Switzerland
[c] Faculty of Engineering, University of Porto (FEUP), Rua Dr. Roberto Frias, s/n, 4200-465 Porto, Portugal

ARTICLE INFO

Article history:
Received 20 June 2015
Accepted 21 August 2015
Available online xxx

Keywords:
Single beacon navigation
AUV trimming trajectories
Set of indistinguishable states
Observability

ABSTRACT

We analyze the observability properties of the kinematic model of an autonomous underwater vehicle (AUV) moving in 3D, under the influence of ocean currents, using range and depth measurements. The results obtained shed light into the types of trajectories that an AUV may be requested to undergo in order to ensure observability, which is a crucial step in the design of single or multiple beacon positioning systems. We assume that the AUV is equipped with two sensor suites: the first computes the distance (range) of the AUV to single or multiple fixed transponders, while the second measures the vehicle's depth. In both situations, the vehicle has access to its heading angle. We further assume that the AUV undergoes maneuvers commonly known as *trimming trajectories*, that are naturally obtained when the inputs (thruster rpms and control surface deflections) are held constant. This is done for two main reasons: (i) the class of trajectories thus generated is sufficiently rich for a vast number of applications and (ii) from an observability-analysis standpoint they lead to mathematical tractability and allow for an intuitive physical interpretation. These facts stand in sharp contrast to common approaches adopted in the literature, where the characterization of trajectories that yield observability is only implicit and defies a simple interpretation.

In the set-up adopted, the trimming trajectories are completely characterized by three variables: (a) linear body speed $\|\mathbf{v}\|$; (b) flight-path angle γ; and (c) yaw rate $\dot{\psi}$. We assume that $\|\mathbf{v}\| > 0$, γ, and $\dot{\psi}$ are constant but otherwise arbitrary (within the constraints of the vehicle capabilities) and examine the observability of the resulting system with the two above mentioned sensor suites. We adopt definitions of observability and weak observability that seek inspiration from those proposed by Herman and Krener (1977) but reflect the fact that we consider specific kinds of maneuvers in 3D.

We start with the single transponder case. For range measurements only, we show that in the absence of ocean currents the 3D kinematic model of an AUV undergoing trimming trajectories with nonzero flight-path angle and yaw rate is observable. In the case of non-zero but known ocean currents, identical results apply subject to the condition that the flight-path angle satisfies a current-related constraint. However, if the current is non-zero and unknown, the model is only weakly observable. The situation changes completely when both range and depth measurements are available. In this case, under the assumption that the yaw rate is different from zero, observability is obtained even when the flight-path angle is zero (vehicle moving in a horizontal plane) and there are non-zero unknown currents. These obvious advantages are lost if yaw rate is equal to zero, for in this case the model is only weakly observable. In all situations where the model is weakly observable we give a complete characterization of the sets of states that are indistinguishable from a given initial state. Finally, we show that the extended model that is obtained by considering multiple (at least two) transponders is observable in all situations if the yaw rate is different from zero.

☆ This work was supported in part by the EC CADDY project (FP7-ICT-2013, Grant Agreement no. 611373) and the FCT [UID/EEA/50009/2013]. The second author benefited from a Ph.D. scholarship of the Foundation for Science and Technology (FCT), Portugal.
☆☆ A preliminary version of this paper appeared in the Proceedings of the IFAC World Congress, Cape Town, South Africa, August 2014.

* Corresponding author.
E-mail addresses: ncrasta@isr.tecnico.ulisboa.pt (N. Crasta), mbayat@isr.tecnico.ulisboa.pt, behzad.bayat@epfl.ch (M. Bayat), pedro.aguiar@fe.up.pt (A.P. Aguiar), antonio@isr.tecnico.ulisboa.pt (A.M. Pascoal).

http://dx.doi.org/10.1016/j.arcontrol.2015.09.009
1367-5788/

1. Introduction

There is currently widespread interest in the development and operation of autonomous underwater vehicles for challenging scientific and commercial applications at sea. One of the key requisites for the execution of such missions is that the vehicles be capable of computing their positions in 3D space. To this effect, a wide range of sensor suites and methods can be used. See for example Kinsey, Eustice, and Whitcomb (2006) and the references therein for a fast paced introduction to this challenging area of research and some of the key technological solutions adopted.

In recent years, motivated by the need to substantially reduce the cost of underwater positioning systems, there has been a flurry of activity on the study of single beacon positioning systems. These have the potential to drastically reduce the complexity of position systems, for they enable a vehicle to find its position in space by using measurements of the successive ranges between the vehicle and a transponder located at a fixed, known position. In spite of significant advances in this area, however much work remains to be done to clarify basic issues related to the observability properties of single or multiple beacon positioning systems. Namely, to characterize the types of vehicle trajectories that render a range-based positioning design model observable. Clearly, this is an important first step in the design of reliable position estimators.

The literature on single beacon positioning, oftentimes referred to as single beacon navigation, is by now quite extensive and defies a simple summary. For this reason, in what follows we give only a brief description of representative work in the area. Different types of models for 2D and 3D single beacon navigation systems have been proposed and the corresponding observability issues have been addressed by resorting to a number of methods that include linearization techniques (Gadre & Stilwell, 2004, 2005) and state-augmentation techniques (Krener & Isidori, 1983), together with differential geometry-based (Arrichiello, Antonelli, Aguiar, & Pascoal, 2011) and algebraic methods (Jouffroy & Reger, 2006).

In Gadre and Stilwell (2004) the authors study the observability of single beacon navigation systems for underwater vehicles evolving in 2D. To this effect, a nonlinear model is adopted where the state vector consists of the vehicle's position and heading, the input vector includes the body's linear and rotational speeds, and the output vector consists of ranges to a fixed beacon and heading. The vehicle's sideslip angle is assumed to be negligible. The nonlinear system is linearized about nominal trajectories and standard linear time-varying (LTV) observability tools are used to analyze the observability properties of the resulting linear model (Rugh, 1996). In Gadre and Stilwell (2005), unknown constant ocean currents are augmented to the state vector and a procedure identical to that in Gadre and Stilwell (2004) is used to study the observability of the ensuing model. Because of the tools used, all results are local in nature.

The work in Arrichiello et al. (2011) addresses observability issues in the context of relative AUV positioning using inter-vehicle range measurements. This is done by exploiting nonlinear observability concepts and resorting to Herman–Krener observability rank conditions of local weak observability (Hermann & Krener, 1977). Two observability metrics, given by the inverse of the minimum singular value and the ratio between the maximum and minimum singular values of an appropriately defined observability matrix are derived for the system under study. The results obtained are validated experimentally in an equivalent single beacon navigation scenario.

The problem of single-beacon navigation is also studied in Jouffroy and Reger (2006). The proposed estimator structure and related observability conditions are derived using nonlinear differential algebraic methods. In Parlangeli and Indiveri (2014), the authors discuss the observability properties of a kinematic model for cooperative underwater vehicles using range measurements. Using a state augmentation technique that seeks inspiration from that in Batista, Silvestre, and Oliveira (2011), the trajectories of the nonlinear systems evolving on $\mathbb{R}^3 \times \mathbb{S}^2$ are lifted into an equivalent linear time varying (LTV) system on $\mathbb{R}^{25}$ and the observability analysis is done in a LTV setting.

Recently, the work reported in Bayat, Crasta, Aguiar, and Pascoal (2015) addresses the problem of range-based Autonomous Underwater Vehicle (AUV) localization in the presence of unknown ocean currents. In the set-up adopted, the AUV is equipped with an Attitude and Heading Reference System (AHRS), a depth sensor, and an acoustic device that provides measurements of its distance to a set of stationary beacons. The number of active beacons is not known in advance and may vary with time. The objective is to simultaneously localize the AUV and the beacons. In the design model the states evolve continuously with time but the range measurements are only available at discrete instants of time, possibly in a non-uniform manner. For trimming or steady-state maneuvers (that correspond to AUV trajectories with constant linear and angular velocities expressed in the body-frame) it is shown that if either the position of one of the beacons or the initial position of the AUV are known, then even without depth information the system is weakly observable (i.e., the set of states that are indistinguishable from a given initial configuration contains only a set of finite isolated points). If depth measurements are also available, then the system is observable even in the presence of unknown constant ocean currents. The theoretical setting adopted borrows also from state augmentation techniques.

In spite of the progress done towards understanding observability issues related to range-based AUV positioning, work is still required to characterize explicitly the types of AUV trajectories that yield global observability. This is a direct consequence of the nonlinear characteristics of the problem at hand, which mandate the use of analysis tools that go beyond those afforded by the theory of observability for linear time invariant (LTI) systems (Rugh, 1996).

The theory of nonlinear observability has received considerable impetus due to the pioneering work of Hermann and Krener (1977). In this seminal work the authors presented the celebrated Herman–Krener algebraic rank condition for weak observability. The drawback of it is that it is only a sufficient condition and, most importantly, it fails to provide any additional insight into the unobservable space when the rank condition fails. We recall that if a nonlinear system is weakly observable at a given initial state in the sense of Herman–Krener, then there exists, for every state in an open neighborhood of the given initial state, a corresponding input that will distinguish it from that initial state. Notice, however that this does not imply the existence of a single admissible input that will be able to so for every state in the neighborhood. Hence, in practice, there is a need to identify a class of admissible inputs (if its exists) with the property that every input has the ability to distinguish every pair of initial configurations through observation of the outputs.

Motivated by the above considerations, in this paper we use the weaker notion of observability introduced in Crasta, Bayat, Aguiar, and Pascoal (2014) to study the observability properties of a 3D underwater vehicle model in the presence of ocean currents, under the assumption that the vehicle can only measure the distances to one or more fixed transponders located at known inertial positions. As in Crasta et al. (2014) we consider the case where the vehicle moves along trimming trajectories characterized by constant linear body speed, flight-path angle, and yaw rate. For a single transponder case, with range measurements only, we show that in the absence of ocean currents the 3D kinematic model of an AUV undergoing trimming trajectories with nonzero flight-path angle and yaw rate is observable. In the case of non-zero but known ocean currents, identical results apply subject to the condition that the flight-path angle satisfies a current-related constraint. However, if the current is non-zero and unknown, the model is only weakly observable. The situation changes completely when both range and depth measurements are available. In this case, under the assumption that the yaw rate is different from

Please cite this article as: N. Crasta et al., Observability analysis of 3D AUV trimming trajectories in the presence of ocean currents using range and depth measurements, Annual Reviews in Control (2015), http://dx.doi.org/10.1016/j.arcontrol.2015.09.009

zero, observability is obtained even when the flight-path angle is zero (vehicle moving in a horizontal plane) and there are non-zero unknown currents. These obvious advantages are lost if the yaw rate is equal to zero, for in this case the model is only weakly observable. In all situations where the model is weakly observable we give a complete characterization of the sets of states that are indistinguishable from a given initial state. Finally, we show that the extended model that is obtained by considering multiple (at least two) transponders is observable in all situations if the yaw rate is different from zero. The envisioned impact of the results obtained is twofold: (i) they afford practitioners rules for the choice of general types of trajectories that a vehicle should perform in order to enhance single/multiple beacon observability properties, and (ii) by providing a complete characterization of the sets of indistinguishable states, they are extremely helpful during the phase of positioning system design by clarifying the number of models to adopt in a multiple model adaptive estimation (MMAE) set-up, along the lines proposed in Bayat and Aguiar (2012) and Bayat et al. (2015).

At this point, it is relevant to point out that some of the observability results derived in the present paper bear resemblance to the results derived by the authors in Bayat et al. (2015) using a different mathematical setting. However, the observability analysis done in the present work (for a larger number of single beacon navigation design models) builds on conceptually simple geometric arguments and as such it departs from other approaches proposed in the literature, including that in Bayat et al. (2015). It is this simplicity that allows us to fully characterize and give intuitive geometric interpretations of the sets of indistinguishable states that are obtained when an AUV undergoes trimming trajectories under a number of conditions that involve the presence of ocean currents and the availability of complementary sensor packages.

The paper is organized as follows. Section 2 introduces some basic notation and mathematical results that will be used in later sections. Section 3 summarizes key definitions of observability in the context of nonlinear systems. Section 4 describes the model adopted for the study of the observability properties of a 3D autonomous underwater vehicle (AUV) model when the vehicle undergoes motions along trimming trajectories, using range and depth measurements. Sections 5, 6, and 7 address the observability properties of the 3D single beacon system model for the trimming trajectories and different sensor suites. Finally, Section 8 discusses the results obtained and introduces some topics that warrant further research effort.

2. Mathematical preliminaries

Given a smooth real-valued function $f : \mathbb{R} \to \mathbb{R}$, we define $f^{(k)} := \frac{d^k f}{dt^k}$ with $f^{(0)} = f$. Given $a, b \in \mathbb{R}$ such that $a^2 + b^2 \neq 0$, we let atan2(b, a) be the unique angle $\theta \in [0, 2\pi)$ satisfying $\sin\theta = a/\sqrt{a^2+b^2}$ and $\cos\theta = b/\sqrt{a^2+b^2}$. Given $a, b \in \mathbb{R}$, we write $a = b \mod 2\pi$ if there exists $k \in \mathbb{Z}$ such that $a = b + 2k\pi$. We denote the Euclidean norm in $\mathbb{R}^3$ by $\|\cdot\|$ and the unit sphere in $\mathbb{R}^3$ by $S^2 := \{\mathbf{x} \in \mathbb{R}^3 : \|\mathbf{x}\| = 1\}$. Further, we denote the 3×3 identity matrix by I_3 and the zero vector or matrix by $\mathbf{0}$. We further denote the elements of the standard bases for $\mathbb{R}^3$ by $\mathbf{e}_1$, $\mathbf{e}_2$, and $\mathbf{e}_3$.

We define the orthonormal vectors $\mathbf{w}(\theta)$ and $\mathbf{w}^\perp(\theta)$ by

$$\mathbf{w}(\theta) := \begin{bmatrix} \cos(\theta) \\ \sin(\theta) \\ 0 \end{bmatrix} \text{ and } \mathbf{w}^\perp(\theta) := \begin{bmatrix} -\sin(\theta) \\ \cos(\theta) \\ 0 \end{bmatrix}. \tag{2.1}$$

The group of special orthogonal matrices in 3-dimensions is represented by SO(3). For every $\mathbf{a} \in \mathbb{R}^3$, $(\mathbf{a}\times)$ is the matrix representation of the linear map $\mathbf{b} \mapsto \mathbf{a} \times \mathbf{b}$, $\mathbf{b} \in \mathbb{R}^3$. Given $\mathbf{a} \in \mathbb{R}^3$ and $\theta \in [0, 2\pi)$, $\mathcal{R}(\mathbf{a}, \theta) \in SO(3)$ denotes the rotation matrix about the axis $\mathbf{a}$ by an angle θ, given by (Murray, Li, and Sastry, 1994, Prop. 2.4)

$$\mathcal{R}(\mathbf{a}, \theta) = I_3 + \sin\theta\,(\mathbf{a}\times) + (1 - \cos\theta)\,(\mathbf{a}\times)^2. \tag{2.2}$$

We parametrize points in S^2 by the map $\mathbf{s}$: $[0, 2\pi] \times [0, \pi] \to S^2$ described by

$$\mathbf{s}(\boldsymbol{\alpha}) := \begin{bmatrix} \cos(\alpha_1)\sin(\alpha_2) \\ \sin(\alpha_1)\sin(\alpha_2) \\ \cos(\alpha_2) \end{bmatrix}, \quad \boldsymbol{\alpha} = (\alpha_1, \alpha_2). \tag{2.3}$$

3. Observability of nonlinear systems

Consider the general nonlinear system

$$\left.\begin{aligned} \dot{\mathbf{x}} &= \mathbf{f}(\mathbf{x}, \mathbf{u}), \\ \mathbf{y} &= \mathbf{h}(\mathbf{x}), \end{aligned}\right\} \tag{3.1}$$

where $\mathbf{x} \in \mathbb{R}^n$ is the state, $\mathbf{u}$ is the input vector taking values in a compact subset Ω of $\mathbb{R}^p$ containing zero in its interior, $\mathbf{f}$ is a complete and smooth vector field on $\mathbb{R}^n$, and the output function $\mathbf{h} : \mathbb{R}^n \to \mathbb{R}^q$ has smooth components. We recall the following definitions from Hermann and Krener (1977). To capture the physical constraints of the underlying system, we assume that $\mathbf{u}$ belongs to a (possibly large) set $\mathcal{U}_{ad}$ of admissible inputs.

Definition 1 (Indistinguishability)**.** Two initial states $\mathbf{z}, \mathbf{z}' \in \mathbb{R}^n$ of (3.1) are *indistinguishable* in $[t_0, t_f)$ if, for every input $\mathbf{u}$ in the set of admissible inputs $\mathcal{U}_{ad}$ the solutions of (3.1) satisfying the initial conditions $\mathbf{x}(t_0) = \mathbf{z}$ and $\mathbf{x}(t_0) = \mathbf{z}'$ produce identical output-time histories in $[t_0, t_f)$.

For every $\mathbf{z} \in \mathbb{R}^n$, let $\mathcal{I}(\mathbf{z}) \subseteq \mathbb{R}^n$ denote the set of all states that are indistinguishable from $\mathbf{z}$. Note that indistinguishability is an equivalence relation.

Definition 2 (Observability)**.** The system (3.1) is *observable at* $\mathbf{z} \in \mathbb{R}^n$ if $\mathcal{I}(\mathbf{z}) = \{\mathbf{z}\}$, and is *observable* if $\mathcal{I}(\mathbf{z}) = \{\mathbf{z}\}$ for every $\mathbf{z} \in \mathbb{R}^n$.

Definition 3 (Weak observability)**.** The system (3.1) is *weakly observable at* $\mathbf{z} \in \mathbb{R}^n$ if $\mathbf{z}$ is an isolated point of $\mathcal{I}(\mathbf{z})$ and is *weakly observable* if it is weakly observable at every $\mathbf{z} \in \mathbb{R}^n$.

It is important to remark that the above definitions, though elegant, may prove to be quite restrictive in a number of applications. To show this, notice that if a system is weakly observable at a point $\mathbf{z} \in \mathbb{R}^n$, then there is an open neighborhood N_z of $\mathbf{z}$ such that every initial condition $\mathbf{z}' \in N_z$ different from $\mathbf{z}$ is distinguishable from $\mathbf{z}$ itself. However, the computation of a particular input that will distinguish $\mathbf{z}$ and $\mathbf{z}'$ may, for a fixed $\mathbf{z}$, depend on the initial condition $\mathbf{z}'$. It is therefore natural to ask whether, for a given system, there is a specific class of admissible inputs that are simple to characterize and yet can be used to distinguish the state $\mathbf{z}$ from any other state $\mathbf{z}' \in N_z$ by forcing the system with a particular, *fixed input* in that class. Here, we are strongly motivated by the concept of uniform universal inputs introduced by Sontag in Sontag and Wang (2008).

As we will show later, the answer to the above question may be affirmative in the context of systems that describe the motions of a large class of autonomous vehicles if the outputs (measurements) are chosen appropriately. In the latter case, there is a reduced class $\mathcal{U}_c \subseteq \mathcal{U}_{ad}$ of admissible inputs, with elements denoted $\mathbf{u}^*$, that can be parameterized in terms of a small number of parameters but are sufficiently general to generate maneuvers of interest in a wide range of applications. One such example consists of AUV trimming trajectories that are obtained by holding the physical inputs to the vehicle constant. As we will show later, such trajectories are fully parametrized by total speed, yaw rate, and flight path angle and correspond to helices in 3D space that may degenerate into circumferences and straight lines (Elgersma, 1988). In the context of this paper, such parameters play the role of inputs to the model adopted for AUV trajectory generation. Interestingly enough, each element in this reduced class of inputs (that generate helicoidal trajectories) is sufficiently rich to yield, under well defined conditions, useful observability properties for the models whose outputs consist of range or range

Please cite this article as: N. Crasta et al., Observability analysis of 3D AUV trimming trajectories in the presence of ocean currents using range and depth measurements, Annual Reviews in Control (2015), http://dx.doi.org/10.1016/j.arcontrol.2015.09.009

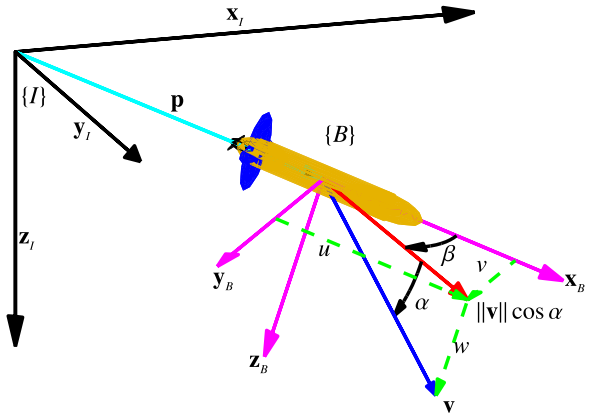

Fig. 1. 3D AUV model for single-beacon navigation.

and depth measurements. This result affords system designers an effective way of selecting simple and yet effective manoeuvres from an observability standpoint. With this motivational background, we recall a weaker notion of observability originally proposed in Crasta et al. (2014) that, as we shall see, will allow for the derivation of observability conditions for the localization system studied in this paper that are easy to interpret physically.

Definition 4 (u*-Indistinguishability)**.** Let $\mathbf{u}^*$ be an admissible input in a given set $\mathcal{U}_c$. We say that two initial states $\mathbf{z}, \mathbf{z}' \in \mathbb{R}^n$ of (3.1) are $\mathbf{u}^*$-*indistinguishable* in $[t_0, t_f)$, if the solutions of (3.1) satisfying the initial conditions $\mathbf{x}(t_0) = \mathbf{z}$ and $\mathbf{x}(t_0) = \mathbf{z}'$ produce identical output-time histories in $[t_0, t_f)$ for $\mathbf{u}^*$.

For every $\mathbf{z} \in \mathbb{R}^n$, let $\mathcal{I}^{\mathbf{u}^*}(\mathbf{z}) \subseteq \mathbb{R}^n$ denote the set of all states that are $\mathbf{u}^*$-indistinguishable from $\mathbf{z}$.

Definition 5 (u*-Observability)**.** The system (3.1) is $\mathbf{u}^*$-*observable at* $\mathbf{z} \in \mathbb{R}^n$ if $\mathcal{I}^{\mathbf{u}^*}(\mathbf{z}) = \{\mathbf{z}\}$, and is *observable* if $\mathcal{I}^{\mathbf{u}^*}(\mathbf{z}) = \{\mathbf{z}\}$ for every $\mathbf{z} \in \mathbb{R}^n$.

Definition 6 (u*-Weak observability)**.** The system (3.1) is $\mathbf{u}^*$-*weakly observable at* $\mathbf{z} \in \mathbb{R}^n$ if $\mathbf{z}$ is an isolated point of $\mathcal{I}^{\mathbf{u}^*}(\mathbf{z})$ and is $\mathbf{u}^*$-*weakly observable* if it is $\mathbf{u}^*$-weakly observable at every $\mathbf{z} \in \mathbb{R}^n$.

Remark 7. Note that observability (O) implies weak observability (WO), while $\mathbf{u}^*$-observability ($\mathbf{u}^*$-O) implies $\mathbf{u}^*$-weak observability ($\mathbf{u}^*$-WO).

4. 3D single-beacon model and trimming trajectories

In what follows, $\{I\}$ and $\{B\}$ denote a inertial and a body-fixed frame with unit vectors $\{\mathbf{x}_I, \mathbf{y}_I, \mathbf{z}_I\}$ and $\{\mathbf{x}_B, \mathbf{y}_B, \mathbf{z}_B\}$, respectively. See Fig. 1. We describe the attitude of an AUV using a matrix $\mathcal{R} \in \mathrm{SO}(3)$ such that the multiplication of $\mathcal{R}$ by a body-fixed vector expresses that vector in the inertial frame. We use the Euler angles of roll (ϕ), pitch (θ), and yaw (ψ) (in this order) to parametrize the matrix $\mathcal{R}$ locally. The kinematic equations that describe the motion of an AUV in $\{I\}$ are given by

$$\left.\begin{aligned} \dot{\mathbf{p}} &= \mathcal{R}_z(\psi)\, \mathcal{R}_y(\theta)\, \mathcal{R}_x(\phi)\, \mathbf{v}, \\ \dot{\boldsymbol{\eta}} &= J(\boldsymbol{\eta})\, \boldsymbol{\omega}, \end{aligned}\right\} \tag{4.1}$$

where $\mathbf{p} \in \mathbb{R}^3$ is the inertial position of the AUV, $\mathbf{v} := (u, v, w) \in \mathbb{R}^3$ is the body-fixed linear velocity vector relative to $\{I\}$ expressed in $\{B\}$, $\boldsymbol{\omega} := (p, q, r) \in \mathbb{R}^3$ is the body-fixed angular velocity vector relative to $\{I\}$ expressed in $\{B\}$, $\boldsymbol{\eta} := (\phi, \theta, \psi) \in [0, 2\pi) \times (-\pi/2, \pi/2) \times [0, 2\pi)$ is the Euler angle vector (roll, pitch, and yaw), $\mathcal{R}_z(\psi) := \mathcal{R}(\mathbf{e}_3, \psi)$, $\mathcal{R}_y(\theta) := \mathcal{R}(\mathbf{e}_2, \theta)$, $\mathcal{R}_x(\phi) := \mathcal{R}(\mathbf{e}_1, \phi)$, and

$$J(\boldsymbol{\eta}) := \begin{bmatrix} 1 & \sin(\phi)\tan(\theta) & \cos(\phi)\tan(\theta) \\ 0 & \cos(\phi) & -\sin(\phi) \\ 0 & \sin(\phi)/\cos(\theta) & \cos(\phi)/\cos(\theta) \end{bmatrix}. \tag{4.2}$$

Following standard nomenclature (Fossen, 1994), the AUV dynamic equations admit the general representation

$$M \begin{bmatrix} \dot{\mathbf{v}} \\ \dot{\boldsymbol{\omega}} \end{bmatrix} + C(\mathbf{v}, \boldsymbol{\omega}) \begin{bmatrix} \mathbf{v} \\ \boldsymbol{\omega} \end{bmatrix} + D(\mathbf{v}, \boldsymbol{\omega}) \begin{bmatrix} \mathbf{v} \\ \boldsymbol{\omega} \end{bmatrix} + g(\boldsymbol{\eta}) = \boldsymbol{\tau}, \tag{4.3}$$

where $M := M_{RB} + M_A$ is the generalized mass matrix of the AUV with M_{RB} and M_A denoting the rigid-body mass matrix and added mass matrix, respectively, $C(\mathbf{v}, \boldsymbol{\omega}) := C_{RB}(\mathbf{v}, \boldsymbol{\omega}) + C_A(\mathbf{v}, \boldsymbol{\omega})$ is the matrix of Coriolis and centripetal terms (including those arising from added mass effects), $D(\mathbf{v}, \boldsymbol{\omega})$ is the hydrodynamic damping matrix, $g(\boldsymbol{\eta})$ is the vector of gravitational/buoyancy forces and moments, and $\boldsymbol{\tau}$ is the vector of control inputs (force and torque due to thrusters and/or control planes).

We now recall the concept of trimming trajectories for a vehicle with motion described by (4.1)–(4.3), see Elgersma (1988). This type of trajectories play an important role in the analysis of flight dynamics (namely in aircraft control) because they correspond to situations where there is a force-moment equilibrium in the body-fixed frame, for a fixed input control configuration. Mathematically, they correspond to the equilibrium points of the dynamic Eq. (4.3) with constant inputs, that is, $\dot{\mathbf{v}} \equiv \mathbf{0}$ and $\dot{\boldsymbol{\omega}} \equiv \mathbf{0}$ for all $t \geq 0$, yielding $\mathbf{v} = \mathbf{v}_e$ and $\boldsymbol{\omega} = \boldsymbol{\omega}_e$, where $\mathbf{v}_e$ and $\boldsymbol{\omega}_e$ (values at equilibrium) are constant.

From the dynamic Eq. (4.3), it follows that all the forces and moments that depend on the linear and rotational velocity vectors are constant, with the exception of the static forces and moments $g(\boldsymbol{\eta})$ that depend on ϕ and θ. Hence, for a given constant input configuration, in order to satisfy Eq. (4.3) it is necessary that $g(\boldsymbol{\eta})$ must be a constant vector, as the linear and angular velocity vectors are constant along trimming trajectories. Now notice that stationarity of $g(\boldsymbol{\eta})$ implies that ϕ and θ are constant, that is, $\phi = \phi_e$ and $\theta = \theta_e$, where ϕ_e and θ_e (values at equilibrium) are constant.

At equilibrium $\dot{\phi} = \dot{\phi}_e = 0$ and $\dot{\theta} = \dot{\theta}_e = 0$, thus implying that $\dot{\boldsymbol{\eta}} = \dot{\psi}\, \mathbf{e}_3$. From Eq. (4.1) $\boldsymbol{\omega} = J(\boldsymbol{\eta})^{-1}\, \dot{\boldsymbol{\eta}}$, from which we may conclude that

$$\boldsymbol{\omega}_e = \dot{\psi} \begin{bmatrix} -\sin(\theta_e) \\ \sin(\phi_e)\cos(\theta_e) \\ \cos(\phi_e)\cos(\theta_e) \end{bmatrix}. \tag{4.4}$$

Notice that the body-fixed trimming angular velocity vector depends on the roll, pitch, and yaw rates. Further, since $\boldsymbol{\omega}_e$ is a constant vector, Eq. (4.4) implies that $\dot{\psi}$ is a constant. In other words, the trimming yaw angle ψ_e is given by

$$\psi_e(t) = r\, t + \psi_0, \tag{4.5}$$

where $r \in \mathbb{R}$ is the constant yaw rate and $\psi_0 \in [0, 2\pi)$ is the initial yaw angle.

Define $\boldsymbol{\xi} := [\xi_1\ \xi_2\ \xi_3]^{\mathrm{T}} = \mathcal{R}_y(\theta_e)\mathcal{R}_x(\phi_e)\, \mathbf{v}_e$ and note that $\boldsymbol{\xi} \in \mathbb{R}^3$ is a constant vector because $\theta_e, \phi_e, \mathbf{v}_e$ are constant. Then, from the linear velocity kinematics transformation (4.1) it follows that

$$\dot{\mathbf{p}}_e = [\mathbf{w}(\mathbf{r}\,\mathbf{t} + \boldsymbol{\psi_0})\ -\mathbf{w}^{\perp}(\mathbf{r}\,\mathbf{t} + \boldsymbol{\psi_0})\, \mathbf{e_3}\, \boldsymbol{\xi} \tag{4.6}$$

where $\mathbf{p}_e$ describes the position of the AUV along a trimming trajectory and $\mathbf{w}(\cdot)$, $\mathbf{w}^{\perp}(\cdot)$ are given by (2.1). Define $\beta, \gamma \in [0, 2\pi)$ as

$$\left.\begin{aligned} \beta &:= \mathrm{atan2}(\xi_2, \xi_1), \\ \gamma &:= \mathrm{atan2}(-\xi_3, \|\boldsymbol{\xi} \times \mathbf{e}_3\|). \end{aligned}\right\} \tag{4.7}$$

It can be shown that β is the angle between the vehicle's heading and the velocity vector heading (that is, the *side-slip angle*) and γ is the angle between the horizontal and the velocity vector (that is, the *trimming flight path angle*). By definition of the atan2 function, note that $\mathrm{atan2}(b, a) = \tan^{-1}(b/a) \in (-\pi/2, \pi/2)$ whenever $a > 0$. Since

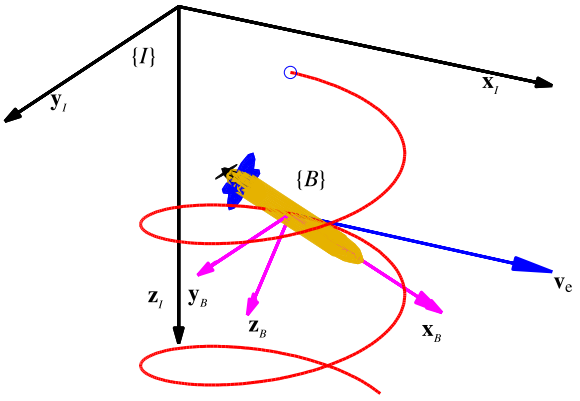

Fig. 2. An AUV trimming trajectory.

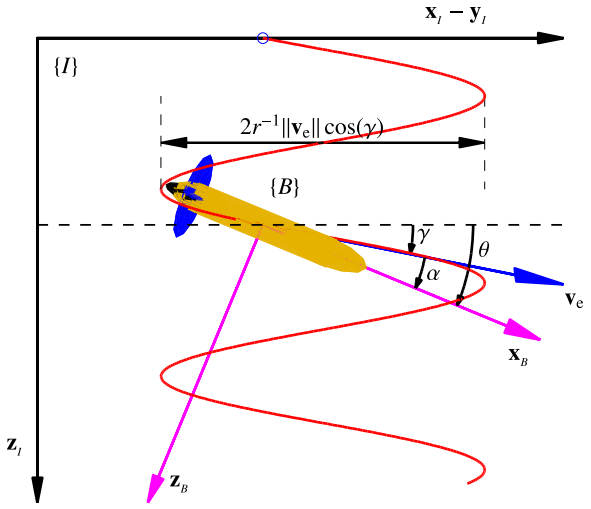

Fig. 3. Trimming trajectory shown in the $\mathbf{x}_B - \mathbf{z}_I$ plane. (γ – flight path angle; θ – pitch angle; α – angle of attack).

$\|\boldsymbol{\xi} \times \mathbf{e}_3\| \geq 0$, from (4.7) we conclude that $\gamma \in [-\pi/2, \pi/2]$. We make the following assumption.

Assumption 8. We assume that $\|\boldsymbol{\xi} \times \mathbf{e}_3\| > 0$, that is, $\gamma \in (-\pi/2, \pi/2)$.

Eq. (4.6) is usually written in the equivalent form

$$\dot{\mathbf{p}}_e = \|\mathbf{v}_e\| \cos(\gamma)\, \mathbf{w}(rt + \psi_0 - \beta) - \|\mathbf{v}_e\| \sin(\gamma)\, \mathbf{e}_3, \tag{4.8}$$

where $\|\mathbf{v}_e\|$ is the linear body speed at trimming. The solution of (4.8) for the initial condition $\mathbf{p}_0 \in \mathbb{R}^3$ is given by

$$\begin{aligned}\mathbf{p}_e(t) - \mathbf{p}_0 = \|\mathbf{v}_e\|\, r^{-1} \,(&-\cos(\gamma)\mathbf{w}^{\perp}(rt + \psi_0 - \beta) \\ &+ \cos(\gamma)\mathbf{w}^{\perp}(\psi_0 - \beta) - \sin(\gamma)\, \mathbf{e}_3\, t),\end{aligned}$$

from which it can be easily concluded that the only trimming trajectories of the underwater vehicle are helices with radii $\|\mathbf{v}_e\|\, r^{-1} \cos(\gamma)$ that may degenerate into straight lines or circumferences. Thus, all trimming trajectories can be parametrized by total vehicle speed, flight path angle, and yaw rate. See Figs. 2 and 3.

In the presence of a constant ocean current $\mathbf{v}_c \in \mathbb{R}^3$, it can be shown that Eq. (4.8) can be rewritten as

$$\dot{\mathbf{p}}_e = \|\mathbf{v}_e\| \cos(\gamma)\, \mathbf{w}(rt + \psi_0 - \beta) - \|\mathbf{v}_e\| \sin(\gamma)\, \mathbf{e}_3 + \mathbf{v}_c \tag{4.9}$$

where $\mathbf{v}_e$ is now the steady state velocity of the vehicle with respect to the fluid and the sideslip β angle is defined accordingly. We remark that in the analysis that follows the dynamics of the AUV don't play any role. They were only introduced to simply show what kind of trimming trajectories an AUV admits in 3D.

Consider now a set of $m(\geq 1)$ transponders located at fixed inertial positions $\mathbf{b}_1, \ldots, \mathbf{b}_m \in \mathbb{R}^3$ with $\mathbf{b}_i \neq \mathbf{b}_j, 1 \leq i, j \leq m, i \neq j$. We assume that the AUV is equipped with a range sensor that measures its distance to these transponders and also a depth sensor. Then, the output (measurement) function is given by

$$\mathbf{y} = \begin{bmatrix} \mathbf{y}_r^{\mathrm{T}} \\ y_d \end{bmatrix}^{\mathrm{T}}$$

where

$$\mathbf{y}_r = \begin{bmatrix} \|\mathbf{p}_e - \mathbf{b}_1\| \\ \vdots \\ \|\mathbf{p}_e - \mathbf{b}_m\| \end{bmatrix}^{\mathrm{T}},$$

$$y_d = \mathbf{e}_3^{\mathrm{T}} \mathbf{p}_e.$$

We consider two cases (i) $m = 1$ and (ii) $m \geq 2$. First we begin with $m = 1$ and characterize the sets of indistinguishable states. Later we extend the characterization in the $m \geq 2$ case using that obtained for the $m = 1$ case. With these characterizations we derive conclusions about the observability/weak observability properties of the single/multiple beacon system for different sensor–actuator configurations.

5. Observability analysis with single beacon

From the results in the previous section, the 3D kinematic model associated with the trimming trajectories of an AUV that measures its distance to a single transponder located at a known position vector $\mathbf{b} \in \mathbb{R}^3$ is given by

$$\left.\begin{aligned} \dot{\mathbf{p}}_e(t) &= \mathbf{g}(\mathbf{v}_e, \gamma, rt + \psi_0, \beta) + \mathbf{v}_c(t), \\ \dot{\mathbf{v}}_c(t) &= \mathbf{0}, \\ y(t) &= \|\mathbf{p}_e(t) - \mathbf{b}\|, \end{aligned}\right\} \tag{5.1}$$

where

$$\mathbf{g}(\mathbf{v}_e, \gamma, rt + \psi_0, \beta) := \|\mathbf{v}_e\| \,(\cos(\gamma)\mathbf{w}(rt + \psi_d) - \sin(\gamma)\mathbf{e}_3), \tag{5.2}$$

$\mathbf{p}_e(t) \in \mathbb{R}^3$ is the inertial position vector, $\mathbf{v}_c(t) \in \mathbb{R}^3$ a constant ocean current disturbance, $\|\mathbf{v}_e\| > 0$ is the linear trimming body speed, $\gamma \in (-\pi/2, \pi/2)$ is the trimming flight path angle, ψ_0 is the initial yaw angle, r is the yaw rate , β is the side-slip angle , and $\psi_d := \psi_0 - \beta$ is the initial heading of the velocity vector. We make the following assumption.

Assumption 9. Without loss of generality, we assume that the beacon is at the origin.

Eq. (5.1) defines a nonlinear input-affine system with state $\mathbf{x} := (\mathbf{p}_e, \mathbf{v}_c) \in \mathbb{R}^3 \times \mathbb{R}^3$, drift vector field $\mathbf{F}(\mathbf{x}) := (\mathbf{v}_c, \mathbf{0})$, control vector field $\mathbf{G}(\mathbf{x}) := (\mathbf{g}, \mathbf{0})$, and output function $h(\mathbf{x}) \in \mathbb{R}$ with $h_1(\mathbf{x}) = \|\mathbf{p}_e\|$. The solution of (5.1) for the initial condition $\mathbf{x}_0 := (\mathbf{p}_0, \mathbf{v}_{c_0}) \in \mathbb{R}^3 \times \mathbb{R}^3$ at time $t \in [0, t_f]$ is denoted by $\Phi_t(\mathbf{x}_0)$ and is given by

$$\Phi_t(\mathbf{x}_0) = \begin{bmatrix} \mathbf{p_0} \\ \mathbf{v}_{c_0} \end{bmatrix} + \begin{bmatrix} \mathbf{v}_{c_0}\, \mathbf{t} + \int_0^{\mathbf{t}} \mathbf{g}(\mathbf{v}_e, \gamma, \mathbf{r}\,\tau + \boldsymbol{\psi_0}, \beta)\, \mathrm{d}\tau \\ \mathbf{0} \end{bmatrix},$$

where the integration in the above equation is the component-wise integration, while the output is given by

$$h_1(\Phi_t(\mathbf{x}_0)) = \left\| \mathbf{p}_0 + \mathbf{v}_{c_0}\, t + \int_0^t \mathbf{g}(\mathbf{v}_e, \gamma, r\,\tau + \psi_0, \beta)\, \mathrm{d}\tau \right\|.$$

For a given $\|\mathbf{v}_e\| > 0$, $\gamma \in (-\pi/2, \pi/2)$, and ψ_0, $\beta \in [0, 2\pi)$ we denote

$$\mathbf{v}_0 := \|\mathbf{v}_e\| \cos(\gamma)\, \mathbf{w}(\psi_d) - \|\mathbf{v}_e\| \sin(\gamma)\, \mathbf{e}_3, \tag{5.3}$$

Please cite this article as: N. Crasta et al., Observability analysis of 3D AUV trimming trajectories in the presence of ocean currents using range and depth measurements, Annual Reviews in Control (2015), http://dx.doi.org/10.1016/j.arcontrol.2015.09.009

where $\mathbf{w}(\cdot)$ is given by (2.1) and $\psi_d = \psi_0 - \beta$. Given $\gamma \in (-\pi/2, \pi/2)$, $\psi_0, \beta \in [0, 2\pi)$, define $t \mapsto \boldsymbol{\kappa}(t)$ by

$$\boldsymbol{\kappa}(t) := \boldsymbol{\kappa}_0 + \boldsymbol{\kappa}_1(t), \tag{5.4}$$

where $\boldsymbol{\kappa}_0 \in \mathbb{R}^3$ and $t \mapsto \boldsymbol{\kappa}_1(t)$ are given by

$$\boldsymbol{\kappa}_0 := \cos(\gamma)\, \mathbf{w}^{\perp}(\psi_d), \tag{5.5}$$

$$\boldsymbol{\kappa}_1(t) := -\cos(\gamma)\, \mathbf{w}^{\perp}(r\,t + \psi_d) - r\, \sin(\gamma)\, \mathbf{e}_3\, t. \tag{5.6}$$

It can be shown that

$$\boldsymbol{\kappa}^{(j)}(t)\big|_{t=0} = r^j\, \boldsymbol{\zeta}_j,\ 1 \le j \le 3, \tag{5.7}$$

and $\boldsymbol{\kappa}^{(4)}(t) = -r^2\, \boldsymbol{\kappa}^{(2)}(t)$, where

$$\boldsymbol{\zeta}_1 := \cos(\gamma)\, \mathbf{w}(\psi_d) - \sin(\gamma)\, \mathbf{e}_3, \tag{5.8}$$

$$\boldsymbol{\zeta}_2 := \cos(\gamma)\, \mathbf{w}^{\perp}(\psi_d), \tag{5.9}$$

$$\boldsymbol{\zeta}_3 := \cos(\gamma)\, \mathbf{w}(\psi_d). \tag{5.10}$$

At this point, we will make use of a result in Crasta, Bayat, Aguiar, and Pascoal (2013) in order to simplify the observability analysis. The result essentially states that the observability properties of the system (5.1) with range squared measurement and range measurement are equivalent.

In this paper we study the observability properties of model (5.1) for two distinct cases with two different sensor suites, namely, (i) known ocean current and (ii) unknown ocean current. In the following sections, we characterize the set of indistinguishable states for cases (i) and (ii). Notice that the observability properties depend on the type of trimming trajectory adopted, that is, we first fix a type of trajectory and then examine the observability of the resulting model in (5.1).

5.1. Known ocean currents

Consider the system in the presence of a known current $\mathbf{v}_c \in \mathbb{R}^3$, that is,

$$\left.\begin{aligned} \dot{\mathbf{p}}_e &= \mathbf{g}(\mathbf{v}_e, \gamma, r\,t + \psi_0, \beta) + \mathbf{v}_c, \\ y &= \|\mathbf{p}_e\|^2, \end{aligned}\right\} \tag{5.11}$$

where $\mathbf{g}(\cdot)$ is given by (5.2). Given $\mathbf{p}_0 \in \mathbb{R}^3$, we let $\mathcal{I}^{z}_{r,kc}(\mathbf{p}_0)$ and $\mathcal{I}^{nz}_{r,kc}(\mathbf{p}_0)$ denote the sets of states that are indistinguishable from the given initial state $\mathbf{p}_0$ under the conditions of zero yaw rate and nonzero constant yaw rate, respectively, for system (5.11). In the above, the subscript 'r' means that only range measurements are available, the subscript 'kc' is the abbreviation of known current, and the superscripts 'z' and 'nz' denote zero and non-zero yaw rate, respectively. We next characterize the above sets.

5.1.1. Zero yaw rate

Let $r = 0$. In this case, for a given $\mathbf{v}_c \in \mathbb{R}^3$, $\gamma \in (-\pi/2, \pi/2)$, $\psi_0, \beta \in [0, 2\pi)$ and initial state $\mathbf{p}_0 \in \mathbb{R}^3$,

$$\Phi_t(\mathbf{p}_0) = \mathbf{p}_0 + \mathbf{v}_{tot}\, t,$$
$$h_1(\Phi_t(\mathbf{p}_0)) = \|\mathbf{p}_0 + \mathbf{v}_{tot}\, t\|^2,$$

where $\mathbf{v}_{tot} := \mathbf{v}_0 + \mathbf{v}_c$, $\mathbf{v}_0 = \|\mathbf{v}_e\| \cos(\gamma)\, \mathbf{w}(\psi_d) - \|\mathbf{v}_e\| \sin(\gamma)\, \mathbf{e}_3$ and $\psi_d = \psi_0 - \beta$. We have the following characterization.

Proposition 10. *Consider $\mathbf{v}_c \in \mathbb{R}^3$, $\|\mathbf{v}_e\| > 0$, $\gamma \in (-\pi/2, \pi/2)$, and $\psi_0, \beta \in [0, 2\pi)$. Then, for every $\mathbf{p}_0 \in \mathbb{R}^3$,*

$$\mathcal{I}^{z}_{r,kc}(\mathbf{p}_0) = \left\{\mathcal{R}(\mathbf{v}_{tot}, \theta)\, \mathbf{p}_0 : \theta \in \mathbb{R}\right\}.$$

Proof. Consider $\mathbf{p}_0 \in \mathbb{R}^3$, $\gamma \in (-\pi/2, \pi/2)$, and $\psi_0, \beta \in [0, 2\pi)$. Let $\mathbf{z} \in \mathbb{R}^3$ be such that $\mathbf{z} \in \mathcal{I}^{z}_{r,kc}(\mathbf{p}_0)$. Then $h_1(\Phi_t(\mathbf{z})) = h_1(\Phi_t(\mathbf{p}_0))$ for all $t \in [0, t_f]$, which implies $\|\mathbf{z}\|^2 = \|\mathbf{p}_0\|^2$ and $\mathbf{z}^{\mathrm{T}}\mathbf{v}_{tot} = \mathbf{p}_0^{\mathrm{T}}\mathbf{v}_{tot}$. These two equations (intersection of a sphere and a plane) represent the circumference given by the loci of points $\mathbf{z} = \mathcal{R}(\mathbf{v}_{tot}, \theta)\, \mathbf{p}_0$, $\theta \in \mathbb{R}$.

To show the reverse inclusion, consider $\mathbf{q} := \mathcal{R}(\mathbf{v}_{tot}, \theta)\, \mathbf{p}_0$, $\theta \in \mathbb{R}$. Using the properties of rotation matrices, note that $\|\mathbf{q}\|^2 = \|\mathbf{p}_0\|^2$ and $\mathbf{q}^{\mathrm{T}}\mathbf{v}_{tot} = \mathbf{p}_0^{\mathrm{T}}\mathbf{v}_{tot}$. Using the two previous facts, it can be shown that $h_1(\Phi_t(\mathbf{q})) = h_1(\Phi_t(\mathbf{p}_0))$ for all $t \in [0, t_f]$. Hence the result follows. □

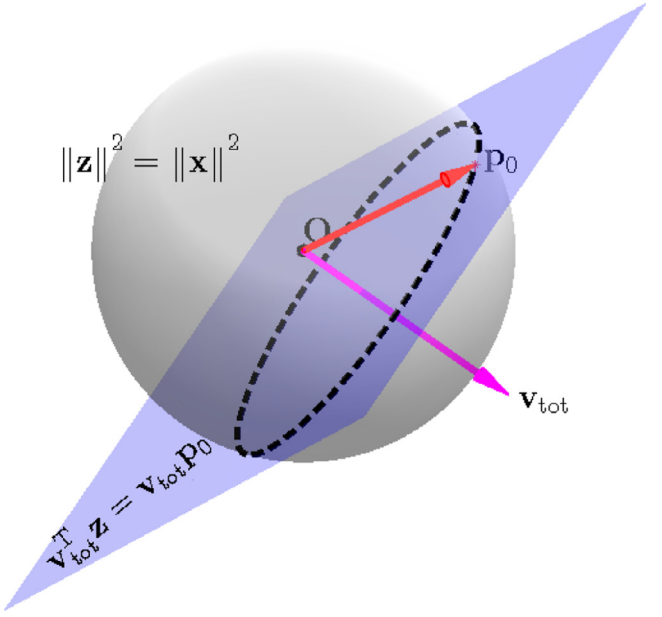

Fig. 4. Geometric visualization of the set $\mathcal{I}^{z}_{r,kc}(\mathbf{p}_0)$.

The following corollary follows immediately from the above proposition.

Corollary 11. *Suppose the beacon is not at the origin, that is, $\mathbf{b} \neq \mathbf{0}$. Then,*

$$\mathcal{I}^{z}_{r,kc}(\mathbf{p}_0) = \left\{\mathbf{b} + \mathcal{R}(\mathbf{v}_{tot}, \theta)\, (\mathbf{p}_0 - \mathbf{b}) : \theta \in \mathbb{R}\right\}.$$

Remark 12. Proposition 10 shows that for a given $\mathbf{p}_0 \in \mathbb{R}^3$ the set of all the points that are obtained by rotating $\mathbf{p}_0$ about the axis $\mathbf{v}_{tot}$ through an arbitrary angle $\theta \in \mathbb{R}$ are indistinguishable.

Remark 13. Note that for a given $\mathbf{p}_0 \in \mathbb{R}^3$ there exist γ, ψ_0, β such that $\mathbf{v}_{tot} \times \mathbf{p}_0 = 0$, that is, $\mathbf{p}_0$ is the eigenvector of $\mathcal{R}(\mathbf{v}_{tot}, \theta)$ corresponding the eigenvalue of $+1$. Consequently, $\mathcal{I}^{z}_{r,kc}(\mathbf{p}_0) = \{\mathbf{p}_0\}$.

Fig. 4 gives a geometrical characterization of the set of states that are indistinguishable from a given initial state $\mathbf{p}_0$.

5.1.2. Nonzero, constant yaw rate

Let $r > 0$. Then for a given $\gamma \in (-\pi/2, \pi/2)$ and $\psi_0, \beta \in [0, 2\pi)$,

$$\Phi_t(\mathbf{p}_0) = \mathbf{p}_0 + \|\mathbf{v}_e\|\, r^{-1}\, \boldsymbol{\kappa}(t) + \mathbf{v}_c\, t,$$
$$h_1(\Phi_t(\mathbf{p}_0)) = \left\|\mathbf{p}_0 + \|\mathbf{v}_e\|\, r^{-1}\, \boldsymbol{\kappa}(t) + \mathbf{v}_c\, t\right\|^2,$$

where $\boldsymbol{\kappa}$ is given by (5.4). We have the following result.

Proposition 14. *Consider $\mathbf{v}_c \in \mathbb{R}^3$, $\|\mathbf{v}_e\|, r > 0$, $\gamma \in (-\pi/2, \pi/2)$, and $\psi_0, \beta \in [0, 2\pi)$. Then, for every $\mathbf{p}_0 \in \mathbb{R}^3$,*

$$\mathcal{I}^{nz}_{r,kc}(\mathbf{p}_0) = \begin{cases} \left\{\mathbf{p}_0, -\mathcal{R}(\mathbf{e}_3, \pi)\, \mathbf{p}_0\right\} & \text{if } \sin(\gamma) = \|\mathbf{v}_e\|^{-1} \mathbf{e}_3^{\mathrm{T}}\mathbf{v}_c, \\ \{\mathbf{p}_0\} & \text{otherwise.} \end{cases}$$

Proof. Consider $\mathbf{p}_0 \in \mathbb{R}^3$, $\gamma \in (-\pi/2, \pi/2)$, $\psi_0, \beta \in [0, 2\pi)$ and $\|\mathbf{v}_e\|$, $r > 0$. Let $\mathbf{z} \in \mathbb{R}^3$ be such that $\mathbf{z} \in \mathcal{I}^{nz}_{r,kc}(\mathbf{p}_0)$. Then, from $h_1(\Phi_t(\mathbf{z})) = h_1(\Phi_t(\mathbf{p}_0))$ for all $t \in [0, t_f]$ it follows that

$$(\|\mathbf{z}\|^2 - \|\mathbf{p}_0\|^2) + 2\, (\mathbf{z} - \mathbf{p}_0)^{\mathrm{T}} \left\{\|\mathbf{v}_e\|\, r^{-1} \boldsymbol{\kappa}(t) + \mathbf{v}_c t\right\} = 0, \tag{5.12}$$

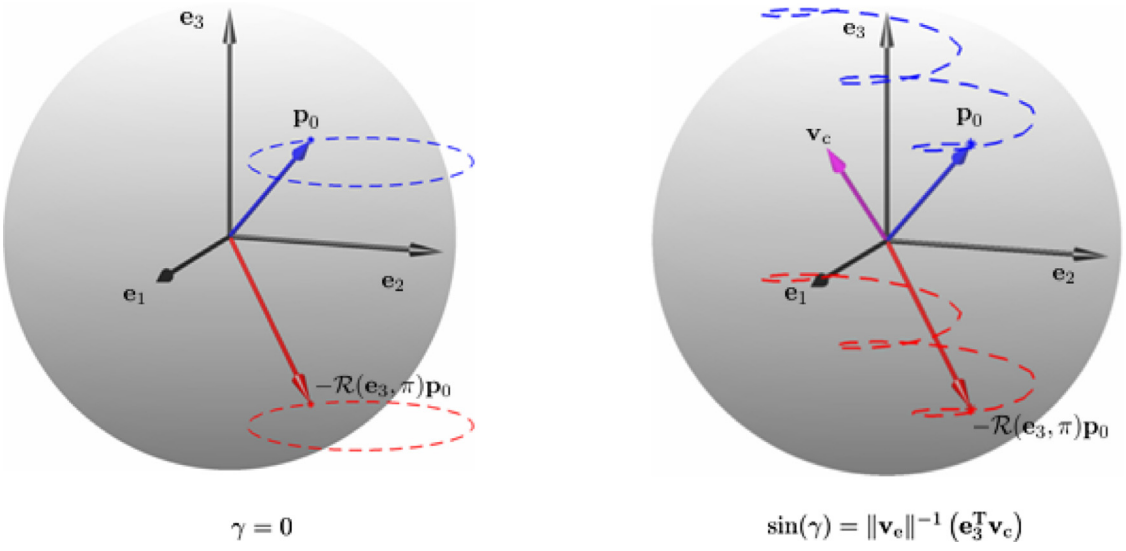

Fig. 5. Geometric visualization of the set $\mathcal{I}^{nz}_{r,kc}(\mathbf{p}_0)$. Left: zero current; Right: known current.

for every $t \in [0, t_f]$. At $t = 0$, the above equation implies that

$$\|\mathbf{z}\|^2 = \|\mathbf{p}_0\|^2. \tag{5.13}$$

Consequently, (5.12) yields

$$(\mathbf{z} - \mathbf{p}_0)^T \left\{ \|\mathbf{v}_e\| r^{-1} \boldsymbol{\kappa}(t) + \mathbf{v}_c t \right\} = 0 \tag{5.14}$$

for every $t \in [0, t_f]$. Since $\|\mathbf{v}_e\|$, γ, r, ψ_v are fixed constants, Eq. (5.14) is only a function of time. Differentiating (5.14) with respect to time and evaluating at $t = 0$ gives

$$(\mathbf{z} - \mathbf{p}_0)^T \left\{ \|\mathbf{v}_e\| r^{-1} \boldsymbol{\kappa}_1^{(1)}(t) + \mathbf{v}_c \right\} \Big|_{t=0} = 0, \tag{5.15}$$

$$(\mathbf{z} - \mathbf{p}_0)^T \boldsymbol{\kappa}_1^{(2)}(t) \Big|_{t=0} = 0, \tag{5.16}$$

$$(\mathbf{z} - \mathbf{p}_0)^T \boldsymbol{\kappa}_1^{(3)}(t) \Big|_{t=0} = 0. \tag{5.17}$$

Furthermore, using (5.7) in (5.15)–(5.17) yields

$$\begin{bmatrix} \{\|\mathbf{v}_e\| \boldsymbol{\zeta}_1 + \mathbf{v}_c\}^T \\ \boldsymbol{\zeta}_2^T \\ \boldsymbol{\zeta}_3^T \end{bmatrix} (\mathbf{z} - \mathbf{p}_0) = 0 \tag{5.18}$$

where the $\boldsymbol{\zeta}_i$'s are given by (5.8)–(5.10). It can be easily verified that $\boldsymbol{\zeta}_2 \times \boldsymbol{\zeta}_3 = -\cos^2(\gamma)\, \mathbf{e}_3$, so that $\boldsymbol{\zeta}_1^T(\boldsymbol{\zeta}_2 \times \boldsymbol{\zeta}_3) = \cos^2(\gamma) \sin(\gamma)$ and $\mathbf{v}_c^T(\boldsymbol{\zeta}_2 \times \boldsymbol{\zeta}_3) = -\cos^2(\gamma)\, \mathbf{e}_3^T\mathbf{v}_c$, and, consequently, $\{\|\mathbf{v}_e\| \boldsymbol{\zeta}_1 + \mathbf{v}_c\}^T(\boldsymbol{\zeta}_2 \times \boldsymbol{\zeta}_3) = \|\mathbf{v}_e\| \cos^2(\gamma) \left[\sin(\gamma) - \delta\right]$, where $\delta := \|\mathbf{v}_e\|^{-1}\mathbf{e}_3^T\mathbf{v}_c$. Since $\gamma \in (-\pi/2, \pi/2)$, it follows that $\cos(\gamma) \neq 0$. Consequently, $\{\|\mathbf{v}_e\| \boldsymbol{\zeta}_1 + \mathbf{v}_c\}^T(\boldsymbol{\zeta}_2 \times \boldsymbol{\zeta}_3) = 0$ if and only if $\sin(\gamma) = \delta$.

(a) First suppose that $\sin(\gamma) \neq \delta$, that is, $\{\|\mathbf{v}_e\| \boldsymbol{\zeta}_1 + \mathbf{v}_c\}^T(\boldsymbol{\zeta}_2 \times \boldsymbol{\zeta}_3) \neq 0$. Then, Eq. (5.18) implies that $\mathbf{z} = \mathbf{p}_0$. The reverse inclusion is trivial. Hence $\mathcal{I}^{nz}_{r,kc}(\mathbf{p}_0) = \{\mathbf{p}_0\}$.

(b) Next suppose that $\sin(\gamma) = \delta$. Note that $\boldsymbol{\zeta}_1 = \boldsymbol{\zeta}_3 - \|\mathbf{v}_e\|^{-1}(\mathbf{e}_3^T\mathbf{v}_c)\, \mathbf{e}_3$, and consequently, $\{\|\mathbf{v}_e\| \boldsymbol{\zeta}_1 + \mathbf{v}_c\}^T(\boldsymbol{\zeta}_2 \times \boldsymbol{\zeta}_3) = 0$. Now (5.18) implies that $\mathbf{z} - \mathbf{p}_0 = \alpha\, (\boldsymbol{\zeta}_2 \times \boldsymbol{\zeta}_3)$, $\alpha \in \mathbb{R}$, that is, $\mathbf{z} = \mathbf{p}_0 - \alpha \cos^2(\gamma)\, \mathbf{e}_3$. Consequently, (5.13) implies that either $\alpha = 0$ or $\alpha = 2\mathbf{e}_3^T\mathbf{p}_0 / \cos^2(\gamma)$. Hence, $\mathbf{z} \in \{\mathbf{p}_0, -\mathcal{R}(\mathbf{e}_3, \pi)\mathbf{p}_0\}$ and $\mathcal{I}^{nz}_{r,kc}(\mathbf{p}_0) \subseteq \{\mathbf{p}_0, -\mathcal{R}(\mathbf{e}_3, \pi)\mathbf{p}_0\}$.

To show the reverse inclusion, consider $\mathbf{q} := -\mathcal{R}(\mathbf{e}_3, \pi)\, \mathbf{p}_0$ and note that $\mathbf{e}_1^T\mathbf{q} = \mathbf{e}_1^T\mathbf{p}_0$, $\mathbf{e}_2^T\mathbf{q} = \mathbf{e}_2^T\mathbf{p}_0$, $\mathcal{R}(\mathbf{e}_3, \pi)^T\boldsymbol{\kappa}_0 = -\boldsymbol{\kappa}_0$, and $\mathcal{R}(\mathbf{e}_3, \pi)^T\boldsymbol{\kappa}_1(t) = -\boldsymbol{\kappa}_1(t) + 2\, \mathbf{e}_3^T\boldsymbol{\kappa}_1(t)\, \mathbf{e}_3$, and consequently, $\mathcal{R}(\mathbf{e}_3, \pi)^T\boldsymbol{\kappa}(t) = -\boldsymbol{\kappa}(t) + 2\, \mathbf{e}_3^T\boldsymbol{\kappa}_1(t)\, \mathbf{e}_3$. With some algebraic manipulations, it can be verified that

$$h_1(\Phi_t(\mathbf{q})) = \left\| -\mathcal{R}(\mathbf{e}_3, \pi) \left\{ \mathbf{p}_0 + \|\mathbf{v}_e\| r^{-1} \boldsymbol{\kappa}(t) + \mathbf{v}_c t \right\} \right\|^2.$$

Using the properties of rotation matrices it now follows that $h_1(\Phi_t(\mathbf{q})) = h_1(\Phi_t(\mathbf{p}_0))$ for all $t \in [0, t_f]$. Consequently, $\{\mathbf{p}_0, -\mathcal{R}(\mathbf{e}_3, \pi)\mathbf{p}_0\} \subseteq \mathcal{I}^{nz}_{r,kc}(\mathbf{p}_0)$ and the result follows. □

The following corollary follows immediately from the above proposition.

Corollary 15. *Suppose the beacon is not at the origin, that is,* $\mathbf{b} \neq \mathbf{0}$. *Then,*

$$\mathcal{I}^{nz}_{r,kc}(\mathbf{p}_0) = \begin{cases} \{\mathbf{p}_0, \mathbf{b} - \mathcal{R}(\mathbf{e}_3, \pi) \\ \quad \times (\mathbf{p}_0 - \mathbf{b})\} & \text{if } \sin(\gamma) = \|\mathbf{v}_e\|^{-1}\mathbf{e}_3^T\mathbf{v}_c, \\ \{\mathbf{p}_0\} & \text{otherwise.} \end{cases}$$

Remark 16. Note that for the system (5.11) in the presence of known currents, a flight path angle satisfying $\sin(\gamma) \neq \|\mathbf{v}_e\|^{-1}\mathbf{e}_3^T\mathbf{v}_c$ yields observability for every nonzero constant yaw rate. In particular, in the absence of currents with nonzero flight path angle system (5.11) is observable for every nonzero constant yaw rate.

Fig. 5 gives a geometrical characterization of the set of states that are indistinguishable from a given initial state $\mathbf{p}_0$.

5.2. Unknown ocean currents

Consider the model of a single-beacon navigation system in the presence of an unknown constant ocean current $\mathbf{v}_c \in \mathbb{R}^3$ described by

$$\left.\begin{aligned} \dot{\mathbf{p}}_e &= \mathbf{g}(\mathbf{v}_e, \gamma, rt + \psi_0, \beta) + \mathbf{v}_c, \\ \dot{\mathbf{v}}_c &= \mathbf{0}, \\ y &= \|\mathbf{p}_e\|^2, \end{aligned}\right\} \tag{5.19}$$

where $\mathbf{g}(\cdot)$ is given by (5.2). Given $(\mathbf{p}_0, \mathbf{v}_{c_0}) \in \mathbb{R}^3 \times \mathbb{R}^3$, we let $\mathcal{I}^{z}_{r,uc}(\mathbf{p}_0, \mathbf{v}_{c_0})$ and $\mathcal{I}^{nz}_{r,uc}(\mathbf{p}_0, \mathbf{v}_{c_0})$ denote the sets of states that are indistinguishable from the given initial state $(\mathbf{p}_0, \mathbf{v}_{c_0})$ for zero yaw rate and nonzero constant yaw rate, respectively, for the system (5.19). In the above, the subscript 'r' means that only range measurements are available, the subscript 'uc' is the abbreviation of unknown current, and the superscripts 'z' and 'nz' denote zero and non-zero yaw rate, respectively. We next characterize $\mathcal{I}^{z}_{r,uc}(\mathbf{p}_0, \mathbf{v}_{c_0})$ and $\mathcal{I}^{nz}_{r,uc}(\mathbf{p}_0, \mathbf{v}_{c_0})$.

Please cite this article as: N. Crasta et al., Observability analysis of 3D AUV trimming trajectories in the presence of ocean currents using range and depth measurements, Annual Reviews in Control (2015), http://dx.doi.org/10.1016/j.arcontrol.2015.09.009

5.2.1. Zero yaw rate

In this case $r = 0$. Consider $\|\mathbf{v}_e\| > 0$, $\gamma \in (-\pi/2, \pi/2)$, $\psi_0, \beta \in [0, 2\pi)$. Then, given an initial condition $(\mathbf{p}_0, \mathbf{v}_{c_0}) \in \mathbb{R}^3 \times \mathbb{R}^3$,

$$\Phi_t(\mathbf{p}_0, \mathbf{v}_{c_0}) = \begin{bmatrix} \mathbf{p_0} \\ \mathbf{v}_{c_0} \end{bmatrix} + \begin{bmatrix} (\mathbf{v}_0 + \mathbf{v}_{c_0})\, t \\ \mathbf{0} \end{bmatrix},$$

$$h_1(\Phi_t(\mathbf{p}_0, \mathbf{v}_{c_0})) \quad = \|\mathbf{p}_0 + (\mathbf{v}_0 + \mathbf{v}_{c_0})\, t\|^2,$$

where $\mathbf{v}_0 \in \mathbb{R}^3$ is given by (5.3). We have the following characterization.

Proposition 17. *Consider $\|\mathbf{v}_e\| > 0$, $\gamma \in (-\pi/2, \pi/2)$, and $\psi_0, \beta \in [0, 2\pi)$. Let $\mathcal{A} := [0, 2\pi] \times [0, \pi]$. Then, given $(\mathbf{p}_0, \mathbf{v}_{c_0}) \in \mathbb{R}^3 \times \mathbb{R}^3$,*

$$\mathcal{I}^z_{r,uc}(\mathbf{p}_0, \mathbf{v}_{c_0}) = \left\{ (\|\mathbf{p}_0\|\, \mathbf{s}(\boldsymbol{\mu}), -\mathbf{v}_0 + \|\mathbf{v}_{tot}\|\, \mathbf{s}(\boldsymbol{\sigma})) : (\boldsymbol{\mu}, \boldsymbol{\sigma}) \in \mathcal{Q} \right\},$$

where $\mathbf{v}_0 \in \mathbb{R}^3$ is given by (5.3), $\mathbf{s}(\cdot)$ is given by (2.3) and

$$\mathbf{v}_{tot} := \mathbf{v}_0 + \mathbf{v}_{c_0},$$

$$\cos(\lambda^*) := \left(\frac{\mathbf{p}_0}{\|\mathbf{p}_0\|}\right)^{\mathrm{T}} \left(\frac{\mathbf{v}_{tot}}{\|\mathbf{v}_{tot}\|}\right),$$

$$\mathcal{Q} := \left\{ (\boldsymbol{\mu}, \boldsymbol{\sigma}) \in \mathcal{A} \times \mathcal{A} : \mathbf{s}(\boldsymbol{\mu})^{\mathrm{T}} \mathbf{s}(\boldsymbol{\sigma}) = \cos(\lambda^*) \right\}.$$

Proof. Consider $\mathbf{x}_0 = (\mathbf{p}_0, \mathbf{v}_{c_0}) \in \mathbb{R}^3 \times \mathbb{R}^3$, $\|\mathbf{v}_e\| > 0$, $\gamma \in (-\pi/2, \pi/2)$, and $\psi_0, \beta \in [0, 2\pi)$. Let $\mathbf{x}_1 = (\mathbf{z}, \mathbf{w}_c) \in \mathbb{R}^3 \times \mathbb{R}^3$ be such that $\mathbf{x}_1 \in \mathcal{I}^z_{r,uc}(\mathbf{x}_0)$. Define $\mathbf{w}_{tot} := \mathbf{v}_0 + \mathbf{w}_c$. Then, $h_1(\Phi_t(\mathbf{x}_1)) = h_1(\Phi_t(\mathbf{x}_0))$ for all $t \in [0, t_f]$ implies that

$$\|\mathbf{z}\|^2 = \|\mathbf{p}_0\|^2, \tag{5.20}$$

$$\|\mathbf{w}_{tot}\|^2 = \|\mathbf{v}_{tot}\|^2, \tag{5.21}$$

$$\mathbf{z}^{\mathrm{T}} \mathbf{w}_{tot} = \mathbf{p}_0^{\mathrm{T}} \mathbf{v}_{tot}. \tag{5.22}$$

Eqs. (5.20) –(5.22) yield

$$\mathbf{z} = \|\mathbf{p}_0\|\, \mathbf{s}(\boldsymbol{\mu}), \tag{5.23}$$

$$\mathbf{w}_c = -\mathbf{v}_0 + \|\mathbf{v}_{tot}\|\, \mathbf{s}(\boldsymbol{\sigma}), \tag{5.24}$$

with $(\boldsymbol{\mu}, \boldsymbol{\sigma}) \in \mathcal{A} \times \mathcal{A}$. Using (5.23) and (5.24) in (5.22), we have $\mathbf{s}(\boldsymbol{\mu})^{\mathrm{T}} \mathbf{s}(\boldsymbol{\sigma}) = \cos(\lambda^*)$. In other words, $(\boldsymbol{\mu}, \boldsymbol{\sigma}) \in \mathcal{Q}$ and hence

$$\mathcal{I}^z_{r,uc}(\mathbf{x}_0) \subseteq \left\{ (\|\mathbf{p}_0\|\, \mathbf{s}(\boldsymbol{\mu}), -\mathbf{v}_0 + \|\mathbf{v}_{tot}\|\, \mathbf{s}(\boldsymbol{\sigma})) : (\boldsymbol{\mu}, \boldsymbol{\sigma}) \in \mathcal{Q} \right\}.$$

Conversely, consider $\mathbf{q} = (\mathbf{q}_1, \mathbf{q}_2)$ where $\mathbf{q}_1 = \|\mathbf{p}_0\|\, \mathbf{s}(\boldsymbol{\mu})$ and $\mathbf{q}_2 = -\mathbf{v}_0 + \|\mathbf{v}_{tot}\|\, \mathbf{s}(\boldsymbol{\sigma})$ for some $(\boldsymbol{\mu}, \boldsymbol{\sigma}) \in \mathcal{Q}$. Note that $\|\mathbf{q}_1\| = \|\mathbf{p}_0\|$ and $\mathbf{v}_0 + \mathbf{q}_2 = \|\mathbf{v}_{tot}\|\, \mathbf{s}(\boldsymbol{\sigma})$. Using these facts, it can be shown that $h_1(\Phi_t(\mathbf{q})) = h_1(\Phi_t(\mathbf{x}_0))$ for all $t \in [0, t_f]$. Consequently,

$$\left\{ (\|\mathbf{p}_0\|\, \mathbf{s}(\boldsymbol{\mu}), -\mathbf{v}_0 + \|\mathbf{v}_{tot}\|\, \mathbf{s}(\boldsymbol{\sigma})) : (\boldsymbol{\mu}, \boldsymbol{\sigma}) \in \mathcal{Q} \right\} \subseteq \mathcal{I}^z_{r,uc}(\mathbf{x}_0).$$

Hence the result follows. □

The following corollary of the above proposition is easily obtained.

Corollary 18. *Suppose the beacon is not at the origin, that is, $\mathbf{b} \neq \mathbf{0}$. Then,*

$$\mathcal{I}^z_{r,uc}(\mathbf{x}_0) = \left\{ (\mathbf{b} + \|\mathbf{p}_0 - \mathbf{b}\|\, \mathbf{s}(\boldsymbol{\mu}), -\mathbf{v}_0 + \|\mathbf{v}_{tot}\|\, \mathbf{s}(\boldsymbol{\sigma})) : (\boldsymbol{\mu}, \boldsymbol{\sigma}) \in \mathcal{Q} \right\},$$

where $\mathbf{x}_0 = (\mathbf{p}_0, \mathbf{v}_{c_0})$, $\mathbf{v}_0 \in \mathbb{R}^3$ is given by (5.3), $\mathbf{s}(\cdot)$ is given by (2.3), and

$$\mathbf{v}_{tot} := \mathbf{v}_0 + \mathbf{v}_{c_0},$$

$$\cos(\lambda^*) := \left(\frac{\mathbf{p}_0 - \mathbf{b}}{\|\mathbf{p}_0 - \mathbf{b}\|}\right)^{\mathrm{T}} \left(\frac{\mathbf{v}_{tot}}{\|\mathbf{v}_{tot}\|}\right),$$

$$\mathcal{Q} := \left\{ (\boldsymbol{\mu}, \boldsymbol{\sigma}) \in \mathcal{A} \times \mathcal{A} : \mathbf{s}(\boldsymbol{\mu})^{\mathrm{T}} \mathbf{s}(\boldsymbol{\sigma}) = \cos(\lambda^*) \right\}.$$

Remark 19. The result above shows that for a given $(\mathbf{p}_0, \mathbf{v}_{c_0}) \in \mathbb{R}^3 \times \mathbb{R}^3$ the set of all the points that are indistinguishable from $(\mathbf{p}_0, \mathbf{v}_{c_0})$ is a lower dimensional surface in $\mathbb{R}^3 \times \mathbb{R}^3$. Consequently, the system is not weakly observable.

5.2.2. Nonzero, constant yaw rate

In this case $r > 0$. Consider $\|\mathbf{v}_e\|$, $r > 0$, $\gamma \in (-\pi/2, \pi/2)$, $\psi_0, \beta \in [0, 2\pi)$. Then, given an initial state $(\mathbf{p}_0, \mathbf{v}_{c_0}) \in \mathbb{R}^3 \times \mathbb{R}^3$,

$$\Phi_t(\mathbf{p}_0, \mathbf{v}_{c_0}) = \begin{bmatrix} \mathbf{p_0} \\ \mathbf{v}_{c_0} \end{bmatrix} + \begin{bmatrix} \|\mathbf{v}_e\|\, r^{-1}\, \boldsymbol{\kappa}(t) + \mathbf{v}_{c_0}\, t \\ \mathbf{0} \end{bmatrix},$$

$$h_1(\Phi_t(\mathbf{p}_0, \mathbf{v}_{c_0})) = \left\| \mathbf{p}_0 + \|\mathbf{v}_e\|\, r^{-1}\, \boldsymbol{\kappa}(t) + \mathbf{v}_{c_0}\, t \right\|^2,$$

where $\boldsymbol{\kappa}$ is given by (5.4). We have the following result.

Proposition 20. *Consider r, $\|\mathbf{v}_e\| > 0$, $\gamma \in (-\pi/2, \pi/2)$, and $\psi_0, \beta \in [0, 2\pi)$. Then, for a given $\mathbf{x}_0 = (\mathbf{p}_0, \mathbf{v}_{c_0}) \in \mathbb{R}^3 \times \mathbb{R}^3$,*

$$\mathcal{I}^{nz}_{r,uc}(\mathbf{x}_0) = \left\{ \mathbf{x}_0, (-\mathcal{R}(\mathbf{e}_3, \pi)\, \mathbf{p}_0, 2\, \|\mathbf{v}_e\|\, \sin(\gamma)\, \mathbf{e}_3 - \mathcal{R}(\mathbf{e}_3, \pi)\, \mathbf{v}_{c_0}) \right\}.$$

Proof. Consider $\mathbf{x}_0 := (\mathbf{p}_0, \mathbf{v}_{c_0}) \in \mathbb{R}^3 \times \mathbb{R}^3$, $\|\mathbf{v}_e\|$, $r > 0$, $\gamma \in (-\pi/2, \pi/2)$, and $\psi_0, \beta \in [0, 2\pi)$. Let $(\mathbf{z}, \mathbf{w}_c) \in \mathbb{R}^3 \times \mathbb{R}^3$ be such that $(\mathbf{z}, \mathbf{w}_c) \in \mathcal{I}^{nz}_{r,uc}(\mathbf{p}_0, \mathbf{v}_{c_0})$. Then, $h_1(\Phi_t(\mathbf{z}, \mathbf{w}_c)) = h_1(\Phi_t(\mathbf{p}_0, \mathbf{v}_{c_0}))$ at $t = 0$ implies

$$\|\mathbf{z}\|^2 = \|\mathbf{p}_0\|^2. \tag{5.25}$$

Define

$$\boldsymbol{\nu}_1(t) := \|\mathbf{v}_e\|\, r^{-1}\, \boldsymbol{\kappa}(t) + \mathbf{w}_c\, t, \tag{5.26}$$

$$\boldsymbol{\nu}_2(t) := \|\mathbf{v}_e\|\, r^{-1}\, \boldsymbol{\kappa}(t) + \mathbf{v}_{c_0}\, t, \tag{5.27}$$

where $\boldsymbol{\kappa}$ is given by (5.4) and note that

$$\boldsymbol{\nu}_1^{(1)}(t) = \|\mathbf{v}_e\|\, r^{-1}\, \boldsymbol{\kappa}^{(1)}(t) + \mathbf{w}_c, \tag{5.28}$$

$$\boldsymbol{\nu}_2^{(1)}(t) = \|\mathbf{v}_e\|\, r^{-1}\, \boldsymbol{\kappa}^{(1)}(t) + \mathbf{v}_{c_0}. \tag{5.29}$$

Consequently, $\boldsymbol{\nu}_1^{(2)}(t) = \boldsymbol{\nu}_2^{(2)}(t) := \|\mathbf{v}_e\|\, r^{-1}\, \boldsymbol{\kappa}^{(1)}(t)$. Using (5.25) in $h_1(\Phi_t(\mathbf{z}, \mathbf{w}_c)) = h_1(\Phi_t(\mathbf{p}_0, \mathbf{v}_{c_0}))$ for all $t \geq 0$, we have

$$\|\boldsymbol{\nu}_2(t)\|^2 + 2\, \mathbf{z}^{\mathrm{T}} \boldsymbol{\nu}_2(t) = \|\boldsymbol{\nu}_1(t)\|^2 + 2\, \mathbf{p}_0^{\mathrm{T}} \boldsymbol{\nu}_1(t), \tag{5.30}$$

for all $t \in [0, t_f]$. The successive time derivatives of (5.30) evaluated at $t = 0$ are given by

$$\mathbf{z}^{\mathrm{T}} \boldsymbol{\nu}_2^{(1)}(0) = \mathbf{p}_0^{\mathrm{T}} \boldsymbol{\nu}_1^{(1)}(0) \tag{5.31}$$

$$\|\boldsymbol{\nu}_2^{(1)}(0)\|^2 + \mathbf{z}^{\mathrm{T}} \boldsymbol{\nu}_1^{(2)}(0) = \|\boldsymbol{\nu}_1^{(1)}(0)\|^2 + \mathbf{p}_0^{\mathrm{T}} \boldsymbol{\nu}_1^{(2)}(0) \tag{5.32}$$

$$3\, \boldsymbol{\nu}_2^{(1)}(0)^{\mathrm{T}} \boldsymbol{\nu}_2^{(2)}(0) + \mathbf{z}^{\mathrm{T}} \boldsymbol{\nu}_1^{(3)}(0) = 3\, \boldsymbol{\nu}_1^{(1)}(0)^{\mathrm{T}} \boldsymbol{\nu}_1^{(2)}(0) + \mathbf{p}_0^{\mathrm{T}} \boldsymbol{\nu}_1^{(3)}(0) \tag{5.33}$$

$$4\, \boldsymbol{\nu}_2^{(1)}(0)^{\mathrm{T}} \boldsymbol{\nu}_2^{(3)}(0) + \mathbf{z}^{\mathrm{T}} \boldsymbol{\nu}_1^{(2)}(0) = 4\, \boldsymbol{\nu}_1^{(1)}(0)^{\mathrm{T}} \boldsymbol{\nu}_1^{(3)}(0) + \mathbf{p}_0^{\mathrm{T}} \boldsymbol{\nu}_1^{(2)}(0) \tag{5.34}$$

$$5\, \boldsymbol{\nu}_2^{(1)}(0)^{\mathrm{T}} \boldsymbol{\nu}_2^{(2)}(0) + \mathbf{z}^{\mathrm{T}} \boldsymbol{\nu}_1^{(3)}(0) = 5\, \boldsymbol{\nu}_1^{(1)}(0)^{\mathrm{T}} \boldsymbol{\nu}_1^{(2)}(0) + \mathbf{p}_0^{\mathrm{T}} \boldsymbol{\nu}_1^{(3)}(0) \tag{5.35}$$

$$6\, \boldsymbol{\nu}_2^{(1)}(0)^{\mathrm{T}} \boldsymbol{\nu}_2^{(3)}(0) + \mathbf{z}^{\mathrm{T}} \boldsymbol{\nu}_1^{(2)}(0) = 6\, \boldsymbol{\nu}_1^{(1)}(0)^{\mathrm{T}} \boldsymbol{\nu}_1^{(3)}(0) + \mathbf{p}_0^{\mathrm{T}} \boldsymbol{\nu}_1^{(2)}(0). \tag{5.36}$$

Eqs. (5.33) and (5.35) imply that

$$\boldsymbol{\nu}_2^{(1)}(0)^{\mathrm{T}} \boldsymbol{\nu}_2^{(2)}(0) = \boldsymbol{\nu}_1^{(1)}(0)^{\mathrm{T}} \boldsymbol{\nu}_1^{(2)}(0), \tag{5.37}$$

while (5.34) and (5.36) yield

$$\boldsymbol{\nu}_2^{(1)}(0)^{\mathrm{T}} \boldsymbol{\nu}_2^{(3)}(0) = \boldsymbol{\nu}_1^{(1)}(0)^{\mathrm{T}} \boldsymbol{\nu}_1^{(3)}(0). \tag{5.38}$$

Since $\boldsymbol{\nu}_2^{(2)}(0) = \boldsymbol{\nu}_1^{(2)}(0)$ and $\boldsymbol{\nu}_2^{(3)}(0) = \boldsymbol{\nu}_1^{(3)}(0)$, it follows from Eqs. (5.37) and (5.38) that

$$\boldsymbol{\nu}_2^{(1)}(0) - \boldsymbol{\nu}_1^{(1)}(0) = \alpha\, (\boldsymbol{\nu}_2^{(2)}(0) \times \boldsymbol{\nu}_2^{(3)}(0)),\ \alpha \in \mathbb{R}. \tag{5.39}$$

Further note that

$$\boldsymbol{\nu}_2^{(2)}(0) = \|\mathbf{v}_e\|\, r\, \cos(\gamma) \mathbf{w}^{\perp}(\psi_0 - \beta),$$

$$\boldsymbol{\nu}_2^{(3)}(0) = -\|\mathbf{v}_e\|\, r^2\, \cos(\gamma) \mathbf{w}(\psi_0 - \beta),$$

and therefore

$$\boldsymbol{\nu}_2^{(2)}(0) \times \boldsymbol{\nu}_2^{(3)}(0) = (\|\mathbf{v}_e\|\, \cos(\gamma))^2\, r^3\, \mathbf{e}_3 \neq 0 \tag{5.40}$$

Please cite this article as: N. Crasta et al., Observability analysis of 3D AUV trimming trajectories in the presence of ocean currents using range and depth measurements, Annual Reviews in Control (2015), http://dx.doi.org/10.1016/j.arcontrol.2015.09.009

Table 1
Observability analysis for zero/nonzero (but constant) yaw rate with range-only measurements in the weaker sense.

System	Zero yaw rate		Nonzero, constant yaw rate	
	$\mathbf{v}_{\text{tot}} \times \mathbf{p}_0 = \mathbf{0}$	$\mathbf{v}_{\text{tot}} \times \mathbf{p}_0 \neq \mathbf{0}$	$\sin(\gamma) = \|\mathbf{v}_c\|^{-1}\mathbf{e}_3^{\mathrm{T}}\mathbf{v}_c$	$\sin(\gamma) \neq \|\mathbf{v}_c\|^{-1}\mathbf{e}_3^{\mathrm{T}}\mathbf{v}_c$
Known current	$\mathbf{u}^*$-O	Not $\mathbf{u}^*$-WO	$\mathbf{u}^*$-WO	$\mathbf{u}^*$-O
Unknown current	Not $\mathbf{u}^*$-WO		$\mathbf{u}^*$- WO	

$\mathbf{u}^*$-O: $\mathbf{u}^*$-Observable and $\mathbf{u}^*$-WO: $\mathbf{u}^*$-Weakly observable.

because $\gamma \in (-\pi/2, \pi/2)$ and $\|\mathbf{v}_e\|$, $r > 0$. It can be easily verified that

$$\mathbf{e}_3^{\mathrm{T}}\boldsymbol{\nu}_2^{(2)}(0) = \mathbf{e}_3^{\mathrm{T}}\boldsymbol{\nu}_2^{(3)}(0) = 0. \tag{5.41}$$

Therefore, using (5.40) in (5.39) yields

$$\boldsymbol{\nu}_2^{(1)}(0) = \boldsymbol{\nu}_1^{(1)}(0) + \alpha\,(\|\mathbf{v}_e\|\cos(\gamma))^2 r^3\,\mathbf{e}_3,\ \alpha \in \mathbb{R}. \tag{5.42}$$

From (5.41) and (5.42), it follows that

$$\boldsymbol{\nu}_2^{(1)}(0)^{\mathrm{T}}\boldsymbol{\nu}_2^{(2)}(0) = \boldsymbol{\nu}_1^{(1)}(0)^{\mathrm{T}}\boldsymbol{\nu}_2^{(2)}(0),$$
$$\boldsymbol{\nu}_2^{(1)}(0)^{\mathrm{T}}\boldsymbol{\nu}_2^{(3)}(0) = \boldsymbol{\nu}_1^{(1)}(0)^{\mathrm{T}}\boldsymbol{\nu}_2^{(3)}(0),$$

and consequently, Eqs. (5.33) and (5.34) imply that

$$\begin{bmatrix}\boldsymbol{\nu}_1^{(2)}(0)^{\mathrm{T}}\\ \boldsymbol{\nu}_1^{(3)}(0)^{\mathrm{T}}\end{bmatrix}(\mathbf{z}-\mathbf{p}_0) = 0, \tag{5.43}$$

that is,

$$\mathbf{z} - \mathbf{p}_0 = \alpha\,(\boldsymbol{\nu}_1^{(2)}(0) \times \boldsymbol{\nu}_1^{(3)}(0)) = \alpha\,[\|\mathbf{v}_e\|\cos(\gamma)]^2 r^3\,\mathbf{e}_3,\ \alpha \in \mathbb{R}.$$

In other words, $\mathbf{z} = \mathbf{p}_0 + \alpha\,(\|\mathbf{v}_e\|^2 r^3\cos^2(\gamma))\,\mathbf{e}_3$. Further, $\|\mathbf{z}\|^2 = \|\mathbf{p}_0\|^2$ implies that either $\alpha = 0$ or $\alpha = -2\,[\|\mathbf{v}_e\|^2 r^3\cos^2(\gamma)]^{-1}\,\mathbf{e}_3^{\mathrm{T}}\mathbf{p}_0$. Note that $\alpha = 0$ implies $\mathbf{z} = \mathbf{p}_0$, while $\alpha = -2\,[\|\mathbf{v}_e\|^2 r^3\cos^2(\gamma)]^{-1}\mathbf{e}_3^{\mathrm{T}}\mathbf{p}_0$ implies $\mathbf{z} = -\mathcal{R}(\mathbf{e}_3, \pi)\mathbf{p}_0$, that is, $\mathbf{z} \in \{\mathbf{p}_0,\ -\mathcal{R}(\mathbf{e}_3, \pi)\mathbf{p}_0\}$.

(i) Suppose first that $\mathbf{z} = \mathbf{p}_0$. Recall that $\boldsymbol{\nu}_2^{(1)}(0) = \boldsymbol{\nu}_1^{(1)}(0) + \alpha\,[\|\mathbf{v}_e\|\cos(\gamma)]^2 r^3\,\mathbf{e}_3$, $\alpha \in \mathbb{R}$. Then, Eq. (5.32) implies that $\|\boldsymbol{\nu}_2^{(1)}(0)\|^2 = \|\boldsymbol{\nu}_1^{(1)}(0)\|^2$, that is, either $\alpha = 0$ or $\alpha = -2\,[\|\mathbf{v}_e\|^2 r^3\cos^2(\gamma)]^{-1}\,\mathbf{e}_3^{\mathrm{T}}\boldsymbol{\nu}_1^{(1)}(0)$.
Further, $\alpha = 0$ implies $\boldsymbol{\nu}_2^{(1)}(0) = \boldsymbol{\nu}_1^{(1)}(0)$, which in turn implies $\mathbf{w}_c = \mathbf{v}_{c_0}$. On the other hand, $\alpha = -2\,[\|\mathbf{v}_e\|^2 r^3\cos^2(\gamma)]^{-1}\,\mathbf{e}_3^{\mathrm{T}}\boldsymbol{\nu}_1^{(1)}(0)$ implies $\boldsymbol{\nu}_2^{(1)}(0) = -\mathcal{R}(\mathbf{e}_3, \pi)\,\boldsymbol{\nu}_1^{(1)}(0)$, which further implies that $\mathbf{w}_c = 2\,\|\mathbf{v}_e\|\sin(\gamma)\,\mathbf{e}_3 - \mathcal{R}(\mathbf{e}_3, \pi)\,\mathbf{v}_{c_0}$, that is, $\mathbf{z}_c \in \{\mathbf{v}_{c_0},\ 2\|\mathbf{v}_e\|\sin(\gamma)\,\mathbf{e}_3 - \mathcal{R}(\mathbf{e}_3, \pi)\,\mathbf{v}_{c_0}\}$.
Now consider $(\mathbf{z}, \mathbf{z}_c) = (\mathbf{p}_0, 2\,\|\mathbf{v}_e\|\sin(\gamma)\,\mathbf{e}_3 - \mathcal{R}(\mathbf{e}_3, \pi)\,\mathbf{v}_{c_0})$. Then,

$$h_1(\Phi_t(\mathbf{z}, \mathbf{z}_c)) = \left\|\mathbf{z} + \|\mathbf{v}_e\|\,r^{-1}\,\boldsymbol{\kappa}(t) + \mathbf{z}_c\,t\right\| \neq h_1(\Phi_t(\mathbf{p}_0, \mathbf{v}_{c_0})).$$

Consequently, $(\mathbf{z}, \mathbf{z}_c) \notin \mathcal{I}^{\text{nz}}_{\text{r,uc}}(\mathbf{p}_0, \mathbf{v}_{c_0})$.

(ii) Suppose next that $\mathbf{z} = -\mathcal{R}(\mathbf{e}_3, \pi)\,\mathbf{p}_0$. Recall that $\boldsymbol{\nu}_2^{(1)}(0) = \boldsymbol{\nu}_1^{(1)}(0) + \alpha\,[\|\mathbf{v}_e\|\cos(\gamma)]^2 r^3\,\mathbf{e}_3$, $\alpha \in \mathbb{R}$. Then, Eq. (5.32) implies that $\|\boldsymbol{\nu}_2^{(1)}(0)\|^2 = \|\boldsymbol{\nu}_1^{(1)}(0)\|^2$, that is, either $\alpha = 0$ or $\alpha = -2\,[\|\mathbf{v}_e\|^2 r^3\cos^2(\gamma)]^{-1}\,\mathbf{e}_3^{\mathrm{T}}\boldsymbol{\nu}_1^{(1)}(0)$.
Further, $\alpha = 0$ implies that $\boldsymbol{\nu}_2^{(1)}(0) = \boldsymbol{\nu}_1^{(1)}(0)$, which in turn implies $\mathbf{w}_c = \mathbf{v}_{c_0}$. On the other hand, $\alpha = -2\,[\|\mathbf{v}_e\|^2 r^3\cos^2(\gamma)]^{-1}\,\mathbf{e}_3^{\mathrm{T}}\boldsymbol{\nu}_1^{(1)}(0)$ implies $\boldsymbol{\nu}_2^{(1)}(0) = -\mathcal{R}(\mathbf{e}_3, \pi)\,\boldsymbol{\nu}_1^{(1)}(0)$, which further implies that $\mathbf{w}_c = 2\|\mathbf{v}_e\|\sin(\gamma)\,\mathbf{e}_3 - \mathcal{R}(\mathbf{e}_3, \pi)\,\mathbf{v}_{c_0}$, that is, $\mathbf{z}_c \in \{\mathbf{v}_{c_0},\ 2\|\mathbf{v}_e\|\sin(\gamma)\,\mathbf{e}_3 - \mathcal{R}(\mathbf{e}_3, \pi)\,\mathbf{v}_{c_0}\}$.
Consider $(\mathbf{z}, \mathbf{z}_{c_0}) = (-\mathcal{R}(\mathbf{e}_3, \pi)\mathbf{p}_0, \mathbf{v}_{c_0})$. Then, one may easily verify that

$$h_1(\Phi_t(\mathbf{z}, \mathbf{z}_{c_0})) = \left\|\mathbf{z} + \|\mathbf{v}_e\|\,r^{-1}\,\boldsymbol{\kappa}(t) + \mathbf{z}_{c_0}\,t\right\| \neq h_1(\Phi_t(\mathbf{p}_0, \mathbf{v}_{c_0})),$$

and consequently, $(\mathbf{z}, \mathbf{z}_{c_0}) \notin \mathcal{I}^{\text{nz}}_{\text{r,uc}}(\mathbf{p}_0, \mathbf{v}_{c_0})$.

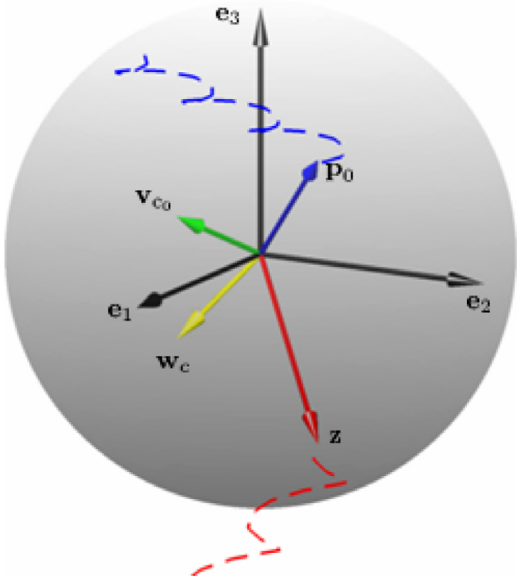

Fig. 6. Geometric visualization of the set $\mathcal{I}^{\text{nz}}_{\text{r,uc}}(\mathbf{p}_0, \mathbf{v}_{c_0})$.

Table 2
Observability analysis for zero and nonzero (but constant) yaw rate with range-only measurements in the Hermann–Krener sense.

System	Zero yaw rate	Nonzero, constant yaw rate
Known current	O	O
Unknown current	Not WO	WO

O: Observable and WO: Weakly observable.

In other words,

$$\mathcal{I}^{\text{nz}}_{\text{r,uc}}(\mathbf{x}_0) \subseteq \left\{\mathbf{x}_0,\ (-\mathcal{R}(\mathbf{e}_3, \pi)\mathbf{p}_0, 2\|\mathbf{v}_e\|\sin(\gamma)\mathbf{e}_3 - \mathcal{R}(\mathbf{e}_3, \pi)\mathbf{v}_{c_0})\right\}.$$

To show the reverse inclusion, consider $(\mathbf{z}, \mathbf{z}_c) = (-\mathcal{R}(\mathbf{e}_3, \pi)\,\mathbf{p}_0, 2\,\|\mathbf{v}_e\|\sin(\gamma)\,\mathbf{e}_3 - \mathcal{R}(\mathbf{e}_3, \pi)\,\mathbf{v}_{c_0})$. Then, it can be shown that $h_1(\Phi_t(\mathbf{z}, \mathbf{z}_c)) = h_1(\Phi_t(\mathbf{p}_0, \mathbf{v}_{c_0}))$ for all $t \geq 0$. Consequently, $(\mathbf{z}, \mathbf{z}_c) \in \mathcal{I}^{\text{nz}}_{\text{r,uc}}(\mathbf{p}_0, \mathbf{v}_{c_0})$. In other words,

$$\left\{\mathbf{x}_0,\ (-\mathcal{R}(\mathbf{e}_3, \pi)\,\mathbf{p}_0, 2\,\|\mathbf{v}_e\|\,\sin(\gamma)\,\mathbf{e}_3 - \mathcal{R}(\mathbf{e}_3, \pi)\,\mathbf{v}_{c_0})\right\} \subseteq \mathcal{I}^{\text{nz}}_{\text{r,uc}}(\mathbf{x}_0).$$

This completes the proof. □

Corollary 21. *Suppose the beacon is not at the origin, that is,* $\mathbf{b} \neq \mathbf{0}$. *Then,*

$$\mathcal{I}^{\text{nz}}_{\text{r,uc}}(\mathbf{x}_0) = \{\mathbf{x}_0,\ (\mathbf{b} - \mathcal{R}(\mathbf{e}_3, \pi)(\mathbf{p}_0 - \mathbf{b}), 2\|\mathbf{v}_e\|\sin(\gamma)\mathbf{e}_3 - \mathcal{R}(\mathbf{e}_3, \pi)\mathbf{v}_{c_0})\}.$$

Remark 22. The system (5.19) with nonzero constant yaw rate is weakly observable.

Fig. 6 depicts the set of states that are indistinguishable from a given initial state $(\mathbf{p}_0, \mathbf{v}_{c_0})$.

Tables 1 and 2 summarize our findings about the observability properties with the range-only output function in the weak notion and the Herman–Krener sense, respectively.

Please cite this article as: N. Crasta et al., Observability analysis of 3D AUV trimming trajectories in the presence of ocean currents using range and depth measurements, Annual Reviews in Control (2015), http://dx.doi.org/10.1016/j.arcontrol.2015.09.009

6. Observability analysis with single range and depth measurements

We now address the case where depth measurements are available. Consider the system in the presence of a known current $\mathbf{v}_c \in \mathbb{R}^3$ given by

$$\dot{\mathbf{p}}_e(t) = \mathbf{g}(\mathbf{v}_e, \gamma, rt + \psi_0, \beta) + \mathbf{v}_c(t), \tag{6.1}$$

$$\dot{\mathbf{v}}_c(t) = \mathbf{0}, \tag{6.2}$$

$$\mathbf{y}(t) = \begin{bmatrix} \|\mathbf{p}_e(t)\|^2 \\ \mathbf{e}_3^{\mathrm{T}}\mathbf{p}_e(t) \end{bmatrix}, \tag{6.3}$$

where $\mathbf{p}_e(t) \in \mathbb{R}^3$ is the inertial position vector, $\mathbf{v}_c(t) \in \mathbb{R}^3$ a constant ocean current disturbance, $\|\mathbf{v}_e\| > 0$ is the linear trimming body speed, $\gamma \in (-\pi/2, \pi/2)$ is the trimming flight path angle, ψ_0 is the initial yaw angle, r is the yaw rate, and β is the side-slip angle.

6.1. Known ocean currents

Consider the system in the presence of a known current $\mathbf{v}_c \in \mathbb{R}^3$, that is,

$$\left.\begin{aligned} \dot{\mathbf{p}}_e &= \mathbf{g}(\mathbf{v}_e, \gamma, rt + \psi_0, \beta) + \mathbf{v}_c, \\ \mathbf{y} &= \begin{bmatrix} \|\mathbf{p}_e\|^2 \\ \mathbf{e}_3^{\mathrm{T}}\mathbf{p}_e \end{bmatrix}, \end{aligned}\right\} \tag{6.4}$$

where $\mathbf{g}(\cdot)$ is given by (5.2). Given $\mathbf{p}_0 \in \mathbb{R}^3$, we let $\mathcal{I}^{z}_{rd,kc}(\mathbf{p}_0)$ and $\mathcal{I}^{nz}_{rd,kc}(\mathbf{p}_0)$ denote the sets of states that are indistinguishable from the given initial state $\mathbf{p}_0$ for zero yaw rate, and nonzero constant yaw rate, respectively, for the system (6.4). In the above, the subscript 'rd' means that both range and depth measurements are available, the subscript 'kc' is the abbreviation of known current, and the superscripts 'z' and 'nz' denote zero and non-zero yaw rate, respectively. We next characterize $\mathcal{I}^{z}_{rd,kc}(\mathbf{p}_0)$ and $\mathcal{I}^{nz}_{rd,kc}(\mathbf{p}_0)$ for the system (6.4).

6.1.1. Zero yaw rate

In this case $r = 0$. Consider $\gamma \in (-\pi/2, \pi/2)$, $\psi_0, \beta \in [0, 2\pi)$ and $\|\mathbf{v}_e\| > 0$. Then, for a given $\mathbf{p}_0 \in \mathbb{R}^3$, we have

$$\begin{aligned} \Phi_t(\mathbf{p}_0) &= \mathbf{p}_0 + \mathbf{v}_{tot}\, t, \\ \mathbf{h}(\Phi_t(\mathbf{p}_0)) &= \begin{bmatrix} \|\mathbf{p}_0 + \mathbf{v}_{tot}\, t\|^2 \\ \mathbf{e}_3^{\mathrm{T}}[\mathbf{p}_0 + \mathbf{v}_{tot}\, t] \end{bmatrix}, \end{aligned}$$

where $\mathbf{v}_{tot} := \mathbf{v}_0 + \mathbf{v}_c$ and $\mathbf{v}_0 \in \mathbb{R}^3$ is given by (5.3).

Proposition 23. *Consider $\mathbf{v}_c \in \mathbb{R}^3$, $\|\mathbf{v}_e\| > 0$, $\gamma \in (-\pi/2, \pi/2)$, and $\psi_0, \beta \in [0, 2\pi)$. Then, for every $\mathbf{p}_0 \in \mathbb{R}^3$,*

$$\mathcal{I}^{z}_{rd,kc}(\mathbf{p}_0) = \begin{cases} \{\mathbf{p}_0\} & \text{if } \mathbf{v}_{tot} \times \mathbf{p}_0 = 0, \\ \{\mathbf{p}_0, \mathcal{R}(\mathbf{v}_{tot}, \theta^*)\mathbf{p}_0\} & \text{otherwise,} \end{cases}$$

where $\mathbf{v}_{tot} := \mathbf{v}_0 + \mathbf{v}_c$ with $\mathbf{v}_0 \in \mathbb{R}^3$ is given by (5.3) and

$$\tan\left(\frac{\theta^*}{2}\right) := -\frac{\mathbf{e}_3^{\mathrm{T}}(\mathbf{v}_{tot} \times \mathbf{p}_0)}{(\mathbf{e}_3 \times \mathbf{v}_{tot})^{\mathrm{T}}(\mathbf{v}_{tot} \times \mathbf{p}_0)}.$$

Proof. Clearly, $\mathcal{I}^{z}_{rd,kc}(\mathbf{p}_0) \subseteq \mathcal{I}^{z}_{r,kc}(\mathbf{p}_0)$. From Proposition 10 recall that

$$\mathcal{I}^{z}_{r,kc}(\mathbf{p}_0) = \left\{\mathcal{R}(\mathbf{v}_{tot}, \theta)\,\mathbf{p}_0 : \theta \in \mathbb{R}\right\}.$$

Let $\mathbf{z} := \mathcal{R}(\mathbf{v}_{tot}, \theta)\,\mathbf{p}_0 \in \mathcal{I}^{z}_{r,kc}(\mathbf{p}_0)$ be such that $\mathbf{z} \in \mathcal{I}^{z}_{rd,kc}(\mathbf{p}_0)$. Then $h_2(\Phi_t(\mathbf{z})) = h_2(\Phi_t(\mathbf{p}_0))$ for all $t \geq 0$, implies

$$\mathbf{e}_3^{\mathrm{T}}\mathbf{z} = \mathbf{e}_3^{\mathrm{T}}\mathbf{p}_0. \tag{6.5}$$

First suppose $\mathbf{v}_{tot} \times \mathbf{p}_0 = 0$. Then $\mathbf{z} = \mathcal{R}(\mathbf{v}_{tot}, \theta)\,\mathbf{p}_0 = \mathbf{p}_0$ and consequently, $\mathcal{I}^{z}_{rd,kc}(\mathbf{p}_0) = \{\mathbf{p}_0\}$. Next suppose $\mathbf{v}_{tot} \times \mathbf{p}_0 \neq 0$. Using (2.2), (6.5) can be written as

$$\sin(\theta)\mathbf{e}_3^{\mathrm{T}}(\mathbf{v}_{tot} \times \mathbf{p}_0) + (1 - \cos(\theta))(\mathbf{e}_3 \times \mathbf{v}_{tot})^{\mathrm{T}}(\mathbf{v}_{tot} \times \mathbf{p}_0) = 0. \tag{6.6}$$

Clearly, $\theta = 2n\pi$ is a trivial solution of this equation. Hence we assume $\theta \neq 2n\pi$. Using the trigonometric identities $\sin(\theta) = 2\sin(\theta/2)\cos(\theta/2)$ and $1 - \cos(\theta) = 2\sin^2(\theta/2)$ along with the fact that $\theta \neq 2n\pi$, Eq. (6.6) yields

$$\tan\left(\frac{\theta^*}{2}\right) = -\frac{\mathbf{e}_3^{\mathrm{T}}(\mathbf{v}_{tot} \times \mathbf{p}_0)}{(\mathbf{e}_3 \times \mathbf{v}_{tot})^{\mathrm{T}}(\mathbf{v}_{tot} \times \mathbf{p}_0)}.$$

We claim that either $\mathbf{e}_3^{\mathrm{T}}(\mathbf{v}_{tot} \times \mathbf{p}_0) \neq 0$ or $(\mathbf{e}_3 \times \mathbf{v}_{tot})^{\mathrm{T}}(\mathbf{v}_{tot} \times \mathbf{p}_0) \neq 0$. To prove the claim suppose $\mathbf{e}_3^{\mathrm{T}}(\mathbf{v}_{tot} \times \mathbf{p}_0) = 0$ and $(\mathbf{e}_3 \times \mathbf{v}_{tot})^{\mathrm{T}}(\mathbf{v}_{tot} \times \mathbf{p}_0) = 0$. This implies

$$\mathbf{e}_3 = k\,\|\mathbf{v}_{tot} \times \mathbf{p}_0\|^2\,\mathbf{v}_{tot},\ k \in \mathbb{R},$$

which is not possible because $\mathbf{v}_{tot} \times \mathbf{p}_0 \neq 0$ and $\gamma \in (-\pi/2, \pi/2)$. Thus, $\tan(\theta/2)$ is well defined.

Further, $\theta = 2n\pi$ implies $\mathbf{z} = \mathcal{R}(\mathbf{v}_{tot}, 2n\pi)\,\mathbf{p}_0 = \mathbf{p}_0$. Suppose $\mathbf{q} := \mathcal{R}(\mathbf{v}_{tot}, \theta^*)\,\mathbf{p}_0$. We have to show that depth information corresponding the trajectories starting from the distinct initial conditions $\mathbf{q}$ and $\mathbf{p}_0$ are identical. By using the trigonometric identities

$$\sin(\theta^*) = \frac{2\tan(\theta^*/2)}{1 + \tan^2(\theta^*/2)}, \tag{6.7}$$

$$\cos(\theta^*) = \frac{1 - \tan^2(\theta^*/2)}{1 + \tan^2(\theta^*/2)}, \tag{6.8}$$

along with Eq. (2.2) one can easily show that

$$\begin{aligned} \mathbf{e}_3^{\mathrm{T}}[\mathbf{z} + \mathbf{v}_{tot}\, t] &= \mathbf{e}_3^{\mathrm{T}}[\mathcal{R}(\mathbf{v}_{tot}, \theta^*)\,\mathbf{p}_0 + \mathbf{v}_{tot}\, t] \\ &= \mathbf{e}_3^{\mathrm{T}}[\mathbf{p}_0 + \sin(\theta^*)\,(\mathbf{v}_{tot} \times \mathbf{p}_0) \\ &\qquad + (1 - \cos(\theta^*))\,(\mathbf{v}_{tot} \times (\mathbf{v}_{tot} \times \mathbf{p}_0)) + \mathbf{v}_{tot}\, t] \\ &= \mathbf{e}_3^{\mathrm{T}}[\mathbf{p}_0 + \mathbf{v}_{tot}\, t]. \end{aligned}$$

Hence the result follows. □

Corollary 24. *Suppose the beacon is not at the origin, that is, $\mathbf{b} \neq \mathbf{0}$. Then,*

$$\mathcal{I}^{z}_{rd,kc}(\mathbf{p}_0) = \begin{cases} \{\mathbf{p}_0\} & \text{if } \mathbf{v}_{tot} \times (\mathbf{p}_0 - \mathbf{b}) = 0, \\ \{\mathbf{p}_0, \mathbf{b} + \mathcal{R}(\mathbf{v}_{tot}, \theta^*) \\ \quad \times(\mathbf{p}_0 - \mathbf{b})\} & \text{otherwise,} \end{cases}$$

where

$$\tan\left(\frac{\theta^*}{2}\right) = -\frac{\mathbf{e}_3^{\mathrm{T}}(\mathbf{v}_{tot} \times (\mathbf{p}_0 - \mathbf{b}))}{(\mathbf{e}_3 \times \mathbf{v}_{tot})^{\mathrm{T}}(\mathbf{v}_{tot} \times (\mathbf{p}_0 - \mathbf{b}))}.$$

Remark 25. Note that for a given $\mathbf{p}_0 \in \mathbb{R}^3$ the system is weakly observable.

6.1.2. Nonzero, constant yaw rate

In this case $r > 0$. Consider $\gamma \in (-\pi/2, \pi/2)$, $\psi_0, \beta \in [0, 2\pi)$ and $\|\mathbf{v}_e\|, r > 0$. Then, for a given $\mathbf{p}_0 \in \mathbb{R}^3$,

$$\begin{aligned} \Phi_t(\mathbf{p}_0) &= \mathbf{p}_0 + \|\mathbf{v}_e\|\, r^{-1}\, \boldsymbol{\kappa}(t) + \mathbf{v}_c\, t, \\ \mathbf{h}(\Phi_t(\mathbf{p}_0)) &= \begin{bmatrix} \left\|\mathbf{p}_0 + \|\mathbf{v}_e\|\, r^{-1}\, \boldsymbol{\kappa}(t) + \mathbf{v}_c\, t\right\|^2 \\ \mathbf{e}_3^{\mathrm{T}}[\mathbf{p}_0 + \|\mathbf{v}_e\|\, r^{-1}\, \boldsymbol{\kappa}(t) + \mathbf{v}_c\, t] \end{bmatrix}, \end{aligned}$$

where $\boldsymbol{\kappa}(t)$ is given by (5.4).

Proposition 26. *Consider $\mathbf{v}_c \in \mathbb{R}^3$, $\|\mathbf{v}_e\|, r > 0$, $\gamma \in (-\pi/2, \pi/2)$ and $\psi_0, \beta \in [0, 2\pi)$. Then, for every $\mathbf{p}_0 \in \mathbb{R}^3$,*

$$\mathcal{I}^{nz}_{rd,kc}(\mathbf{p}_0) = \{\mathbf{p}_0\}.$$

Proof. Consider $\mathbf{v}_c \in \mathbb{R}^3$, $\|\mathbf{v}_e\|, r > 0$, $\gamma \in (-\pi/2, \pi/2)$ and $\psi_0, \beta \in [0, 2\pi)$. From Proposition 14, recall that

$$\mathcal{I}^{\rm nz}_{\rm rd,kc}(\mathbf{p}_0) = \begin{cases} \{\mathbf{p}_0, -\mathcal{R}(\mathbf{e}_3,\pi)\,\mathbf{p}_0\} & \text{if } \sin(\gamma) = \|\mathbf{v}_{\rm e}\|^{-1}\mathbf{e}_3^{\rm T}\mathbf{v}_{\rm c}, \\ \{\mathbf{p}_0\} & \text{otherwise.} \end{cases}$$

and note that $\mathcal{I}^{\rm nz}_{\rm rd,kc}(\mathbf{p}_0) \subseteq \mathcal{I}^{\rm nz}_{\rm r,kc}(\mathbf{p}_0)$. Let $\mathbf{z} \in \mathcal{I}^{\rm nz}_{\rm r,kc}(\mathbf{p}_0)$ be such that $\mathbf{z} \in \mathcal{I}^{\rm nz}_{\rm rd,kc}(\mathbf{p}_0)$. Then $\mathbf{h}(\Phi_t(\mathbf{z})) = \mathbf{h}(\Phi_t(\mathbf{p}_0))$ for all $t \in [0, t_f]$.

Consider $\mathbf{z} = -\mathcal{R}(\mathbf{e}_3,\pi)\,\mathbf{p}_0 \in \mathcal{I}^{\rm nz}_{\rm r,kc}(\mathbf{p}_0)$ and suppose that $\sin(\gamma) = \|\mathbf{v}_{\rm e}\|^{-1}\mathbf{e}_3^{\rm T}\mathbf{v}_{\rm c}$. Notice that $\mathbf{e}_3^{\rm T}\mathbf{p}_0 = 0$ implies that $\mathbf{z} = \mathbf{p}_0$. Hence we assume $\mathbf{e}_3^{\rm T}\mathbf{p}_0 \neq 0$. Now $h_2(\Phi_t(\mathbf{z})) = h_2(\Phi_t(\mathbf{p}_0))$ for all $t \in [0, t_f]$ implies that $\mathbf{e}_3^{\rm T}\mathbf{p}_0 = 0$, which is a contradiction. Hence $\mathcal{I}^{\rm nz}_{\rm rd,kc}(\mathbf{p}_0) = \{\mathbf{p}_0\}$ and the result follows. □

The following corollary follows immediately from the above proposition.

Corollary 27. *Suppose the beacon is not at the origin, that is,* $\mathbf{b} \neq \mathbf{0}$. *Then,*

$$\mathcal{I}^{\rm nz}_{\rm rd,kc}(\mathbf{p}_0) = \{\mathbf{p}_0\}.$$

6.2. Unknown ocean currents

Consider the system in the presence of an unknown constant ocean current $\mathbf{v}_{\rm c} \in \mathbb{R}^3$ described by

$$\left.\begin{aligned} \dot{\mathbf{p}}_{\rm e} &= \mathbf{g}(\mathbf{v}_{\rm e}, \gamma, r\,t + \psi_0, \beta) + \mathbf{v}_{\rm c}, \\ \dot{\mathbf{v}}_{\rm c} &= \mathbf{0}, \\ \mathbf{y} &= \begin{bmatrix} \|\mathbf{p}_{\rm e}\|^2 \\ \mathbf{e}_3^{\rm T}\mathbf{p}_{\rm e} \end{bmatrix}, \end{aligned}\right\} \tag{6.9}$$

where $\mathbf{g}(\cdot)$ is given by (5.2). Given $\mathbf{x}_0 := (\mathbf{p}_0, \mathbf{v}_{\rm c_0}) \in \mathbb{R}^3 \times \mathbb{R}^3$, we let $\mathcal{I}^{\rm z}_{\rm rd,uc}(\mathbf{x}_0)$ and $\mathcal{I}^{\rm nz}_{\rm rd,uc}(\mathbf{x}_0)$ denote the set of states that are indistinguishable from the given initial state $\mathbf{x}_0$ for zero yaw rate and nonzero constant yaw rate, respectively, for the system (6.9). In the above, the subscript 'rd' means that both range and depth measurements are available, the subscript 'uc' is the abbreviation of unknown current, and the superscripts 'z' and 'nz' denote zero and non-zero yaw rate, respectively. We next characterize $\mathcal{I}^{\rm z}_{\rm rd,uc}(\mathbf{x}_0)$ and $\mathcal{I}^{\rm nz}_{\rm rd,uc}(\mathbf{x}_0)$.

6.2.1. Zero yaw rate

Let $r = 0$. For a given $\gamma \in (-\pi/2, \pi/2)$, $\psi_0, \beta \in [0, 2\pi)$ and initial condition $(\mathbf{p}_0, \mathbf{v}_{\rm c_0}) \in \mathbb{R}^3 \times \mathbb{R}^3$, we have

$$\Phi_t(\mathbf{p}_0, \mathbf{v}_{\rm c_0}) = \mathbf{p}_0 + (\mathbf{v}_0 + \mathbf{v}_{\rm c_0})\,t,$$

$$\mathbf{h}(\Phi_t(\mathbf{p}_0, \mathbf{v}_{\rm c_0})) = \begin{bmatrix} \|\mathbf{p}_0 + (\mathbf{v}_0 + \mathbf{v}_{\rm c_0})\,t\|^2 \\ \mathbf{e}_3^{\rm T}[\mathbf{p}_0 + (\mathbf{v}_0 + \mathbf{v}_{\rm c_0})\,t] \end{bmatrix},$$

where $\mathbf{v}_0 \in \mathbb{R}^3$ is given by (5.3).

Proposition 28. *Consider* $\|\mathbf{v}_{\rm e}\| > 0$, $\gamma \in (-\pi/2, \pi/2)$, *and* $\psi_0, \beta \in [0, 2\pi)$. *Then, for a given* $\mathbf{x}_0 := (\mathbf{p}_0, \mathbf{v}_{\rm c_0}) \in \mathbb{R}^3 \times \mathbb{R}^3$,

$$\mathcal{I}^{\rm z}_{\rm rd,3}(\mathbf{x}_0) = \big\{(\|\mathbf{p}_0\|\,\mathbf{s}(\boldsymbol{\mu}^+), -\mathbf{v}_0 + \|\mathbf{v}_{\rm tot}\|\,\mathbf{s}(\boldsymbol{\sigma})) : \sigma \in [0, 2\pi]\big\} \bigcup \big\{(\|\mathbf{p}_0\|\,\mathbf{s}(\boldsymbol{\mu}^-), -\mathbf{v}_0 + \|\mathbf{v}_{\rm tot}\|\,\mathbf{s}(\boldsymbol{\sigma})) : \sigma \in [0, 2\pi]\big\},$$

where $\boldsymbol{\mu}^+ := (\mu^*, \mu_+)$, $\boldsymbol{\mu}^- := (\mu^*, \mu_-)$, $\boldsymbol{\sigma} := (\sigma^*, \sigma)$, $\mathbf{v}_0 \in \mathbb{R}^3$ *is given by (5.3),* $\mathbf{s}(\cdot)$ *is given by (2.3) and*

$$\begin{aligned} \mathbf{v}_{\rm tot} &:= \mathbf{v}_0 + \mathbf{v}_{\rm c_0}, \\ \cos(\lambda^*) &:= \big(\|\mathbf{p}_0\|^{-1}\mathbf{p}_0\big)^{\rm T}\big(\|\mathbf{v}_{\rm tot}\|^{-1}\mathbf{v}_{\rm tot}\big), \\ \cos(\mu^*) &:= \|\mathbf{p}_0\|^{-1}\mathbf{e}_3^{\rm T}\mathbf{p}_0, \\ \cos(\sigma^*) &:= \|\mathbf{v}_{\rm tot}\|^{-1}\mathbf{e}_3^{\rm T}\mathbf{v}_{\rm tot}, \\ \mu_+ &:= (\sigma + \Lambda) \mod 2\pi, \\ \mu_- &:= (\sigma - \Lambda) \mod 2\pi, \\ \Lambda &:= \cos^{-1}\left(\frac{\cos(\lambda^*) - \cos(\mu^*)\cos(\sigma^*)}{\sin(\mu^*)\,\sin(\sigma^*)}\right). \end{aligned}$$

Proof. Consider $\mathbf{x}_0 := (\mathbf{p}_0, \mathbf{v}_{\rm c_0}) \in \mathbb{R}^3 \times \mathbb{R}^3$, $\|\mathbf{v}_{\rm e}\|$, $r > 0$, $\gamma \in (-\pi/2, \pi/2)$, and ψ_0, $\beta \in [0, 2\pi)$. Recall $\mathcal{I}^{\rm z}_{\rm rd,uc}(\mathbf{x}_0) \subseteq \mathcal{I}^{\rm z}_{\rm r,uc}(\mathbf{x}_0)$. Let $\mathbf{x}_1 := (\mathbf{z}, \mathbf{w}_{\rm c}) \in \mathcal{I}^{\rm z}_{\rm rd,uc}(\mathbf{x}_0)$ be such that $\mathbf{x}_1 \in \mathcal{I}^{\rm z}_{\rm r,uc}(\mathbf{x}_0)$. Then, for every $t \in [0, t_f]$,

$$\begin{aligned} h_1(\Phi_t(\mathbf{x}_1)) &= h_1(\Phi_t(\mathbf{x}_0)), \\ h_2(\Phi_t(\mathbf{x}_1)) &= h_2(\Phi_t(\mathbf{x}_0)). \end{aligned}$$

Clearly $h_1(\Phi_t(\mathbf{x}_1)) = h_1(\Phi_t(\mathbf{x}_0))$ for every $t \in [0, t_f]$. From Proposition 17, recall that

$$\mathcal{I}^{\rm z}_{\rm r,uc}(\mathbf{x}_0) = \big\{(\|\mathbf{p}_0\|\,\mathbf{s}(\boldsymbol{\mu}), -\mathbf{v}_0 + \|\mathbf{v}_{\rm tot}\|\,\mathbf{s}(\boldsymbol{\sigma})) : (\boldsymbol{\mu}, \boldsymbol{\sigma}) \in \mathcal{Q}\big\},$$

where

$$\mathcal{Q} := \big\{(\boldsymbol{\mu}, \boldsymbol{\sigma}) \in \mathcal{A} \times \mathcal{A} : \mathbf{s}(\boldsymbol{\mu})^{\rm T}\mathbf{s}(\boldsymbol{\sigma}) = \cos(\lambda^*)\big\}.$$

Consider $(\mathbf{z}, \mathbf{w}_{\rm c}) = (\|\mathbf{p}_0\|\,\mathbf{s}(\boldsymbol{\mu}), -\mathbf{v}_0 + \|\mathbf{v}_{\rm tot}\|\,\mathbf{s}(\boldsymbol{\sigma}))$ for some $(\boldsymbol{\mu}, \boldsymbol{\sigma}) \in \mathcal{Q}$. Then, $h_2(\Phi_t(\mathbf{z}, \mathbf{w}_{\rm c})) = h_2(\Phi_t(\mathbf{x}_0))$ for all $t \in [0, t_f]$ implies that

$$\mathbf{e}_3^{\rm T}\mathbf{z} = \mathbf{e}_3^{\rm T}\mathbf{p}_0, \tag{6.10}$$

$$\mathbf{e}_3^{\rm T}\mathbf{w}_{\rm tot} = \mathbf{e}_3^{\rm T}\mathbf{v}_{\rm tot}, \tag{6.11}$$

where $\mathbf{w}_{\rm tot} = \mathbf{v}_0 + \mathbf{w}_{\rm c}$ and $\mathbf{v}_{\rm tot} = \mathbf{v}_0 + \mathbf{v}_{\rm c_0}$. From Eqs. (6.10) and (6.11) it follows that

$$\cos(\mu_1^*) = \|\mathbf{p}_0\|^{-1}\mathbf{e}_3^{\rm T}\mathbf{p}_0, \tag{6.12}$$

$$\cos(\sigma_1^*) = \|\mathbf{v}_{\rm tot}\|^{-1}\mathbf{e}_3^{\rm T}\mathbf{v}_{\rm tot}. \tag{6.13}$$

On the other hand, $\mathbf{s}(\boldsymbol{\mu})^{\rm T}\mathbf{s}(\boldsymbol{\sigma}) = \cos(\lambda^*)$ implies

$$\cos(\mu_2 - \sigma_2) = \frac{\cos(\lambda^*) - \cos(\mu_1^*)\cos(\sigma_1^*)}{\sin(\mu_1^*)\,\sin(\sigma_1^*)}.$$

Invoking a standard result in elementary trigonometry, we conclude that $\mu_2^1 = (\sigma_2 + \Lambda) \mod 2\pi$ and $\mu_2^2 = (\sigma_2 - \Lambda) \mod 2\pi$, where

$$\Lambda := \cos^{-1}\left(\frac{\cos(\lambda^*) - \cos(\mu_1^*)\cos(\sigma_1^*)}{\sin(\mu_1^*)\,\sin(\sigma_1^*)}\right).$$

In other words,

$$\begin{aligned} \mathcal{I}^{\rm z}_{\rm rd,uc}(\mathbf{x}_0) \subseteq{}& \big\{\big(\|\mathbf{p}_0\|\mathbf{s}(\mu_1^*, \mu_2^1), -\mathbf{v}_0 + \|\mathbf{v}_{\rm tot}\|\mathbf{s}(\sigma_1^*, \sigma_2)\big) : \sigma_2 \in [0, 2\pi]\big\} \\ &\bigcup \big\{\big(\|\mathbf{p}_0\|\mathbf{s}(\mu_1^*, \mu_2^2), -\mathbf{v}_0 + \|\mathbf{v}_{\rm tot}\|\mathbf{s}(\sigma_1^*, \sigma_2)\big) : \sigma_2 \in [0, 2\pi]\big\}. \end{aligned}$$

To show the converse, first consider $\mathbf{q} = (\mathbf{q}_1, \mathbf{q}_2)$ where $\mathbf{q}_1 = \|\mathbf{p}_0\|\mathbf{s}(\mu_1^*, \mu_2^1)$, and $\mathbf{q}_2 = -\mathbf{v}_0 + \|\mathbf{v}_0 + \mathbf{v}_{\rm c_0}\|\mathbf{s}(\sigma_1^*, \sigma_2)$ for some $\sigma_2 \in [0, 2\pi]$. Note that $\|\mathbf{q}_1\| = \|\mathbf{p}_0\|$ and $\mathbf{v}_0 + \mathbf{q}_2 = \|\mathbf{v}_0 + \mathbf{v}_{\rm c_0}\|\,\mathbf{s}(\sigma_1^*, \sigma_2)$. Using these results, it can be shown that $\mathbf{h}(\Phi_t(\mathbf{q})) = \mathbf{h}(\Phi_t(\mathbf{x}_0))$ for all $t \in [0, t_f]$.

Next consider $\bar{\mathbf{q}} = (\bar{\mathbf{q}}_1, \bar{\mathbf{q}}_2)$ where $\bar{\mathbf{q}}_1 = \|\mathbf{p}_0\|\mathbf{s}(\mu_1^*, \mu_2^2)$ and $\bar{\mathbf{q}}_2 = -\mathbf{v}_0 + \|(\mathbf{v}_0 + \mathbf{v}_{\rm c_0})\|\mathbf{s}(\sigma_1^*, \sigma_2)$ for some $\sigma_2 \in [0, 2\pi]$. Note that $\|\bar{\mathbf{q}}_1\| = \|\mathbf{p}_0\|$ and $\mathbf{v}_0 + \bar{\mathbf{q}}_2 = \|\mathbf{v}_0 + \mathbf{v}_{\rm c_0}\|\,\mathbf{s}(\sigma_1^*, \sigma_2)$. Using these facts, it can be shown that $\mathbf{h}(\Phi_t(\bar{\mathbf{q}})) = \mathbf{h}(\Phi_t(\mathbf{x}_0))$ for all $t \in [0, t_f]$. □

The following corollary follows immediately from the above proposition.

Corollary 29. *Suppose the beacon is not at the origin, that is,* $\mathbf{b} \neq \mathbf{0}$. *Then,*

$$\mathcal{I}^{\rm z}_{\rm rd,uc}(\mathbf{x}_0) = \big\{(\|\mathbf{p}_0\|\,\mathbf{s}(\boldsymbol{\mu}^+), -\mathbf{v}_0 + \|\mathbf{v}_{\rm tot}\|\,\mathbf{s}(\boldsymbol{\sigma})) : \sigma \in [0, 2\pi]\big\} \bigcup \big\{(\|\mathbf{p}_0\|\,\mathbf{s}(\boldsymbol{\mu}^-), -\mathbf{v}_0 + \|\mathbf{v}_{\rm tot}\|\,\mathbf{s}(\boldsymbol{\sigma})) : \sigma \in [0, 2\pi]\big\},$$

where $\boldsymbol{\mu}^+ := (\mu^*, \mu_+)$, $\boldsymbol{\mu}^- := (\mu^*, \mu_-)$, $\boldsymbol{\sigma} := (\sigma^*, \sigma)$, $\mathbf{v}_0 \in \mathbb{R}^3$ *is given by (5.3),* $\mathbf{s}(\cdot)$ *is given by (2.3) and*

$$\begin{aligned} \mathbf{v}_{\rm tot} &:= \mathbf{v}_0 + \mathbf{v}_{\rm c_0}, \\ \cos(\lambda^*) &:= \big(\|\mathbf{p}_0 - \mathbf{b}\|^{-1}(\mathbf{p}_0 - \mathbf{b})\big)^{\rm T}\big(\|\mathbf{v}_{\rm tot}\|^{-1}\mathbf{v}_{\rm tot}\big), \end{aligned}$$

$$\cos(\mu^*) := \|\mathbf{p}_0 - \mathbf{b}\|^{-1}\mathbf{e}_3^{\mathrm{T}}(\mathbf{p}_0 - \mathbf{b}),$$
$$\cos(\sigma^*) := \|\mathbf{v}_{\mathrm{tot}}\|^{-1}\mathbf{e}_3^{\mathrm{T}}\mathbf{v}_{\mathrm{tot}},$$
$$\mu_+ := (\sigma + \Lambda) \mod 2\pi,$$
$$\mu_- := (\sigma - \Lambda) \mod 2\pi,$$
$$\Lambda := \cos^{-1}\left(\frac{\cos(\lambda^*) - \cos(\mu^*)\cos(\sigma^*)}{\sin(\mu^*)\sin(\sigma^*)}\right).$$

6.2.2. Nonzero, constant yaw rate

Let $r > 0$. Consider $\gamma \in (-\pi/2, \pi/2)$, ψ_0, $\beta \in [0, 2\pi)$ and $\|\mathbf{v}_e\| > 0$. Then, for a given initial condition $\mathbf{x}_0 := (\mathbf{p}_0, \mathbf{v}_{c_0}) \in \mathbb{R}^3 \times \mathbb{R}^3$, we have

$$\Phi_t(\mathbf{x}_0) = \mathbf{p}_0 + \|\mathbf{v}_e\| r^{-1} \boldsymbol{\kappa}(t) + \mathbf{v}_{c_0} t,$$
$$\mathbf{h}(\Phi_t(\mathbf{x}_0)) = \begin{bmatrix} \left\|\mathbf{p}_0 + \|\mathbf{v}_e\| r^{-1} \boldsymbol{\kappa}(t) + \mathbf{v}_{c_0} t\right\|^2 \\ \mathbf{e}_3^{\mathrm{T}}[\mathbf{p}_0 + \|\mathbf{v}_e\| r^{-1} \boldsymbol{\kappa}(t) + \mathbf{v}_{c_0} t] \end{bmatrix},$$

where $\boldsymbol{\kappa}(t)$ is given by (5.4).

Proposition 30. *Consider* $\|\mathbf{v}_e\|$, $r > 0$, $\gamma \in (-\pi/2, \pi/2)$, *and* ψ_0, $\beta \in [0, 2\pi)$. *Then, for every* $(\mathbf{p}_0, \mathbf{v}_{c_0}) \in \mathbb{R}^3 \times \mathbb{R}^3$, $\mathcal{I}^{\mathrm{nz}}_{\mathrm{rd,uc}}(\mathbf{p}_0, \mathbf{v}_{c_0}) = \{(\mathbf{p}_0, \mathbf{v}_{c_0})\}$.

Proof. Consider $\mathbf{x}_0 := (\mathbf{p}_0, \mathbf{v}_{c_0}) \in \mathbb{R}^3 \times \mathbb{R}^3$, $\|\mathbf{v}_e\|$, $r > 0$, $\gamma \in (-\pi/2, \pi/2)$, and ψ_0, $\beta \in [0, 2\pi)$. Recall $\mathcal{I}^{\mathrm{nz}}_{\mathrm{rd,uc}}(\mathbf{x}_0) \subseteq \mathcal{I}^{\mathrm{nz}}_{\mathrm{r,uc}}(\mathbf{x}_0)$. Let $\mathbf{x}_1 := (\mathbf{z}, \mathbf{w}_c) \in \mathcal{I}^{\mathrm{nz}}_{\mathrm{r,uc}}(\mathbf{x}_0)$ be such that $\mathbf{x}_1 \in \mathcal{I}^{\mathrm{nz}}_{\mathrm{rd,uc}}(\mathbf{x}_0)$. Then, for every $t \in [0, t_f]$,

$$h_1(\Phi_t(\mathbf{x}_1)) = h_1(\Phi_t(\mathbf{x}_0)),$$
$$h_2(\Phi_t(\mathbf{x}_1)) = h_2(\Phi_t(\mathbf{x}_0)).$$

Clearly $h_1(\Phi_t(\mathbf{x}_1)) = h_1(\Phi_t(\mathbf{x}_0))$ for every $t \in [0, t_f]$. From Proposition 20, recall that

$$\mathcal{I}^{\mathrm{nz}}_{\mathrm{r,uc}}(\mathbf{x}_0) = \{(\mathbf{p}_0, \mathbf{v}_{c_0}), (-\mathcal{R}(\mathbf{e}_3, \pi)\,\mathbf{p}_0, 2\|\mathbf{v}_e\| \sin(\gamma)\,\mathbf{e}_3 - \mathcal{R}(\mathbf{e}_3, \pi)\,\mathbf{v}_{c_0})\}.$$

Suppose $(\mathbf{z}, \mathbf{w}_c) := (-\mathcal{R}(\mathbf{e}_3, \pi)\,\mathbf{p}_0, 2\|\mathbf{v}_e\| \sin(\gamma)\,\mathbf{e}_3 - \mathcal{R}(\mathbf{e}_3, \pi)\,\mathbf{v}_{c_0}) \in \mathcal{I}^{\mathrm{nz}}_{\mathrm{r,uc}}(\mathbf{x}_0)$. Then,

$$\begin{aligned} h_2(\Phi_t(\mathbf{z}, \mathbf{w}_c)) &= \mathbf{e}_3^{\mathrm{T}}[\mathbf{z} + \|\mathbf{v}_e\| r^{-1} \boldsymbol{\kappa}(t) + \mathbf{w}_c t] \\ &= \mathbf{e}_3^{\mathrm{T}}[-\mathcal{R}(\mathbf{e}_3, \pi)\mathbf{p}_0 + \|\mathbf{v}_e\| r^{-1} \boldsymbol{\kappa}(t) \\ &\quad + \|\mathbf{v}_e\| \sin(\gamma)\mathbf{e}_3 t - \mathcal{R}(\mathbf{e}_3, \pi)\mathbf{v}_{c_0} t] \\ &= \mathbf{e}_3^{\mathrm{T}}[-\mathbf{p}_0 + \|\mathbf{v}_e\| r^{-1} \boldsymbol{\kappa}(t) + \|\mathbf{v}_e\| \sin(\gamma)\mathbf{e}_3 t - \mathbf{v}_{c_0} t] \\ &= -h_2(\Phi_t(\mathbf{x}_0)) + \|\mathbf{v}_e\| \sin(\gamma)\, t + \|\mathbf{v}_e\| r^{-1}\, \mathbf{e}_3^{\mathrm{T}} \boldsymbol{\kappa}(t) \\ &\neq h_2(\Phi_t(\mathbf{x}_0)). \end{aligned}$$

Consequently, $(\mathbf{z}, \mathbf{w}_c) \notin \mathcal{I}^{\mathrm{nz}}_{\mathrm{rd,uc}}(\mathbf{x}_0)$. This completes the proof. □

The following corollary follows immediately from the above proposition.

Corollary 31. *Suppose the beacon is not at the origin, that is,* $\mathbf{b} \neq \mathbf{0}$. *Then,*

$$\mathcal{I}^{\mathrm{nz}}_{\mathrm{rd,uc}}(\mathbf{p}_0, \mathbf{v}_{c_0}) = \{(\mathbf{p}_0, \mathbf{v}_{c_0})\}.$$

Table 3 summarizes our findings with range and depth as output functions, whereas Table 4 provides a summary of observability properties in the Herman–Krener sense.

7. Observability analysis with multiple beacons

In this section we extend the observability analysis of Section 5 to multiple transponders. We make use of the characterization of indistinguishable states in Section 5 to draw stronger conclusions in this section.

Table 3
Observability analysis for zero and nonzero (but constant) yaw rate with range-only measurements in the weaker sense.

System	Zero yaw rate		Nonzero, constant yaw rate
	$\mathbf{v}_{\mathrm{tot}} \times \mathbf{p}_0 = \mathbf{0}$	$\mathbf{v}_{\mathrm{tot}} \times \mathbf{p}_0 \neq \mathbf{0}$	
Known current	$\mathbf{u}^*$-O	Not $\mathbf{u}^*$-WO	$\mathbf{u}^*$- O
Unknown current	Not $\mathbf{u}^*$-WO		$\mathbf{u}^*$-O

$\mathbf{u}^*$-O: $\mathbf{u}^*$-Observable and $\mathbf{u}^*$-WO: $\mathbf{u}^*$-Weakly observable.

Table 4
Observability analysis for zero and nonzero (but constant) yaw rate with range and depth measurements, in the Hermann–Krener sense.

System	Zero yaw rate	Nonzero, constant yaw rate
Known current	O	O
Unknown current	Not WO	O

O: Observable and WO: Weakly observable.

Consider a set of $m(\geq 2)$ transponders located at fixed inertial positions $\mathbf{B} = \{\mathbf{b}_1, \ldots, \mathbf{b}_m\} \subset \mathbb{R}^3$ with $\mathbf{b}_k \neq \mathbf{b}_l$, $1 \leq k, l \leq m$. In this case, the corresponding output function is given by

$$\mathbf{y} = \begin{bmatrix} \|\mathbf{p}_e - \mathbf{b}_1\|^2 \\ \vdots \\ \|\mathbf{p}_e - \mathbf{b}_m\|^2 \end{bmatrix}. \tag{7.1}$$

For the sake of clarity, we denote the set of indistinguishable states with respect to the i^{th} beacon $\mathbf{b}_i$ by ${}_{\mathbf{b}_i}\mathcal{I}^*_{*,**}(\mathbf{p}_0)$, whereas ${}_{\mathbf{B}}\mathcal{I}^*_{*,**}(\mathbf{p}_0)$ denotes the sets of indistinguishable states with respect to all the beacons. In the above the superscript refers to the situation of zero/nonzero yaw rate, the subscript '$*$' refers to the availability of range/range and depth measurements, and the subscript '$**$' denotes the case of known/unknown current. Clearly,

$${}_{\mathbf{B}}\mathcal{I}^*_{\mathrm{r},*}(\mathbf{p}_0) = \bigcap_{1 \leq i \leq m} {}_{\mathbf{b}_i}\mathcal{I}^*_{\mathrm{r},*}(\mathbf{p}_0). \tag{7.2}$$

In general, with more than four transponders it is possible to achieve observability. However our next results show that with less than four transponders it is possible to achieve observability with the aid of depth information.

7.1. Knownocean currents

In this section, under some mild conditions, we show that observability can be achieved with at least two transponders for any constant yaw rate. However, the zero yaw rate case requires depth information.

7.1.1. Zero yaw rate

In this case, one can clearly obtain observability with four transponders using trilateration. However, with depth measurements, it is possible to achieve observability with two distinct transponders.

Proposition 32. *Let* $m \geq 2$ *and assume that the depth information is accessible. Consider* $\mathbf{v}_c \in \mathbb{R}^3$, $\|\mathbf{v}_e\| > 0$, $\gamma \in (-\pi/2, \pi/2)$, *and* $\psi_0, \beta \in [0, 2\pi)$. *Suppose there exist distinct* $i, j \in \{1, \ldots, m\}$ *such that*

$$(\mathbf{b}_j - \mathbf{b}_i)^{\mathrm{T}}(\mathbf{v}_{\mathrm{tot}} \times \mathbf{e}_3) \neq 0.$$

Then, for every $\mathbf{p}_0 \in \mathbb{R}^3$,

$${}_{\mathbf{B}}\mathcal{I}^{\mathrm{z}}_{\mathrm{rd,kc}}(\mathbf{p}_0) = \{\mathbf{p}_0\}.$$

Proof. Let $\bar{\mathbf{p}} \in \mathbb{R}^3$, $\bar{\mathbf{p}} \neq \mathbf{p}_0$, be such that $\bar{\mathbf{p}} \in {}_{\mathbf{B}}\mathcal{I}^{\mathrm{z}}_{\mathrm{rd,kc}}(\mathbf{p}_0)$. Then, for each s, $1 \leq s \leq m$,

$$\|\bar{\mathbf{p}} + \mathbf{v}_{\mathrm{tot}}\, t - \mathbf{b}_s\|^2 = \|\mathbf{p}_0 + \mathbf{v}_{\mathrm{tot}}\, t - \mathbf{b}_s\|^2, \tag{7.3}$$

$$\mathbf{e}_3^{\mathrm{T}}(\bar{\mathbf{p}} + \mathbf{v}_{\mathrm{tot}}\, t - \mathbf{b}_s) = \mathbf{e}_3^{\mathrm{T}}(\mathbf{p}_0 + \mathbf{v}_{\mathrm{tot}}\, t - \mathbf{b}_s), \tag{7.4}$$

which implies that

$$\|\bar{\mathbf{p}} - \mathbf{b}_s\|^2 = \|\mathbf{p}_0 - \mathbf{b}_s\|^2, \tag{7.5}$$

$$\mathbf{v}_{\mathrm{tot}}^{\mathrm{T}}(\bar{\mathbf{p}} - \mathbf{b}_s) = \mathbf{v}_{\mathrm{tot}}^{\mathrm{T}}(\mathbf{p}_0 - \mathbf{b}_s), \tag{7.6}$$

$$\mathbf{e}_3^{\mathrm{T}}(\bar{\mathbf{p}} - \mathbf{b}_s) = \mathbf{e}_3^{\mathrm{T}}(\mathbf{p}_0 - \mathbf{b}_s), \tag{7.7}$$

where $\mathbf{v}_{\mathrm{tot}} = \mathbf{v}_0 + \mathbf{v}_{\mathrm{c}}$ and $\mathbf{v}_0$ is given by (5.3). Let $i, j \in \{1, \ldots, m\}$ be such that $\mathbf{b}_i \neq \mathbf{b}_j$ and $(\mathbf{b}_j - \mathbf{b}_i)^{\mathrm{T}}(\mathbf{v}_{\mathrm{tot}} \times \mathbf{e}_3) \neq 0$. Then, Eq. (7.5) yields

$$\|\bar{\mathbf{p}} - \mathbf{b}_i\|^2 = \|\mathbf{p}_0 - \mathbf{b}_i\|^2, \tag{7.8}$$

$$\|\bar{\mathbf{p}} - \mathbf{b}_j\|^2 = \|\mathbf{p}_0 - \mathbf{b}_j\|^2. \tag{7.9}$$

Taking the difference of the above two equations we obtain

$$(\mathbf{b}_j - \mathbf{b}_i)^{\mathrm{T}}\bar{\mathbf{p}} = (\mathbf{b}_j - \mathbf{b}_i)^{\mathrm{T}}\mathbf{p}_0. \tag{7.10}$$

Eqs. (7.6), (7.7) and (7.10) yield

$$\begin{bmatrix} (\mathbf{b}_j - \mathbf{b}_i)^{\mathrm{T}} \\ \mathbf{v}_{\mathrm{tot}}^{\mathrm{T}} \\ \mathbf{e}_3^{\mathrm{T}} \end{bmatrix} \bar{\mathbf{p}} = \begin{bmatrix} (\mathbf{b}_j - \mathbf{b}_i)^{\mathrm{T}} \\ \mathbf{v}_{\mathrm{tot}}^{\mathrm{T}} \\ \mathbf{e}_3^{\mathrm{T}} \end{bmatrix} \mathbf{p}_0. \tag{7.11}$$

By hypothesis the coefficient matrix is invertible and consequently $\bar{\mathbf{p}} = \mathbf{p}_0$. □

7.1.2. Nonzero, constant yaw rate

The following result shows that with at least two distinct transponders at different depths, observability can be achieved for nonzero yaw rate in the presence of a known current.

Proposition 33. *Consider* $m \geq 2$, $\mathbf{v}_{\mathrm{c}} \in \mathbb{R}^3$, $\|\mathbf{v}_{\mathrm{e}}\|$, $r > 0$, $\gamma \in (-\pi/2, \pi/2)$, *and* ψ_0, $\beta \in [0, 2\pi)$. *Suppose there exists* $k, l \in \{1, \ldots, m\}$ *such that* $\mathbf{e}_3^{\mathrm{T}}(\mathbf{b}_k - \mathbf{b}_l) \neq 0$. *Then, for every* $\mathbf{p}_0 \in \mathbb{R}^3$

$${}_{\mathbf{B}}\mathcal{I}^{\mathrm{nz}}_{\mathrm{r,kc}}(\mathbf{p}_0) = \{\mathbf{p}_0\}.$$

Proof. For every $i \in \{1, \ldots, m\}$, Corollary 15 implies that

$${}_{\mathbf{b}_i}\mathcal{I}^{\mathrm{nz}}_{\mathrm{r,kc}}(\mathbf{p}_0) = \begin{cases} \{\mathbf{p}_0, \mathbf{b}_i - \mathcal{R}(\mathbf{e}_3, \pi) \\ \quad \times (\mathbf{p}_0 - \mathbf{b}_i)\} & \text{if } \sin(\gamma) = \dfrac{\mathbf{e}_3^{\mathrm{T}}\mathbf{v}_{\mathrm{c}}}{\|\mathbf{v}_{\mathrm{e}}\|}, \\ \{\mathbf{p}_0\} & \text{otherwise.} \end{cases}$$

Note that if $\sin(\gamma) \neq \|\mathbf{v}_{\mathrm{e}}\|^{-1}\mathbf{e}_3^{\mathrm{T}}\mathbf{v}_{\mathrm{c}}$, then ${}_{\mathbf{b}_i}\mathcal{I}^{\mathrm{nz}}_{\mathrm{r,kc}}(\mathbf{p}_0) = \{\mathbf{p}_0\}$ and consequently ${}_{\mathbf{B}}\mathcal{I}^{\mathrm{z}}_{\mathrm{r,kc}}(\mathbf{p}_0) = \{\mathbf{p}_0\}$. Hence we assume $\sin(\gamma) \neq \|\mathbf{v}_{\mathrm{e}}\|^{-1}\mathbf{e}_3^{\mathrm{T}}\mathbf{v}_{\mathrm{c}}$. Then, ${}_{\mathbf{b}_i}\mathcal{I}^{\mathrm{nz}}_{\mathrm{r,kc}}(\mathbf{p}_0) = \{\mathbf{p}_0, \mathbf{b}_i - \mathcal{R}(\mathbf{e}_3, \pi)(\mathbf{p}_0 - \mathbf{b}_i)\}$. Further, it can be easily verified that $\mathbf{p}_0 = \mathbf{b}_k - \mathcal{R}(\mathbf{e}_3, \pi)(\mathbf{p}_0 - \mathbf{b}_k)$ for all k implies $\mathbf{b}_k - \mathbf{b}_l = 0$, $\forall\, k \neq l$, while $\mathbf{b}_k - \mathcal{R}(\mathbf{e}_3, \pi)(\mathbf{p}_0 - \mathbf{b}_k) = \mathbf{b}_l - \mathcal{R}(\mathbf{e}_3, \pi)(\mathbf{p}_0 - \mathbf{b}_l)$ implies $\mathbf{e}_3^{\mathrm{T}}(\mathbf{b}_k - \mathbf{b}_l) = 0$, for all $k \neq l$, which is a contradiction. Hence

$${}_{\mathbf{B}}\mathcal{I}^{\mathrm{nz}}_{\mathrm{r,kc}}(\mathbf{p}_0) = \bigcap_{1 \leq i \leq m} {}_{\mathbf{b}_i}\mathcal{I}^{\mathrm{nz}}_{\mathrm{r,kc}}(\mathbf{p}_0) = \{\mathbf{p}_0\}.$$

□

7.2. Unknown ocean currents

In this section we show, under some mild conditions, that observability can be achieved with at least two transponders for nonzero constant yaw rate. However, the zero yaw rate case requires at least three transponders as well as depth information.

7.2.1. Zero yaw rate

Proposition 34. *Let* $m \geq 3$ *and assume that the depth information is available. Consider* $(\mathbf{p}_0, \mathbf{v}_{\mathrm{c}_0}) \in \mathbb{R}^3 \times \mathbb{R}^3$. *Suppose there exist distinct* $i, j, k \in \{1, \ldots, m\}$ *such that*

$$\mathbf{e}_3^{\mathrm{T}}((\mathbf{b}_i - \mathbf{b}_j) \times (\mathbf{b}_j - \mathbf{b}_k)) \neq 0, \tag{7.12}$$

$$\mathbf{e}_3^{\mathrm{T}}((\mathbf{p}_0 - \mathbf{b}_j) \times (\mathbf{p}_0 - \mathbf{b}_j)) \neq 0. \tag{7.13}$$

Consider $\mathbf{v}_{\mathrm{c}} \in \mathbb{R}^3$, $\|\mathbf{v}_{\mathrm{e}}\| > 0$, $\gamma \in (-\pi/2, \pi/2)$, *and* ψ_0, $\beta \in [0, 2\pi)$. *Then,*

$${}_{\mathbf{B}}\mathcal{I}^{\mathrm{z}}_{\mathrm{rd,uc}}(\mathbf{p}_0, \mathbf{v}_{\mathrm{c}_0}) = \{(\mathbf{p}_0, \mathbf{v}_{\mathrm{c}_0})\}. \tag{7.14}$$

Proof. Let $(\bar{\mathbf{p}}, \bar{\mathbf{v}}_{\mathrm{c}}) \in \mathbb{R}^3 \times \mathbb{R}^3$, $(\bar{\mathbf{p}}, \bar{\mathbf{v}}_{\mathrm{c}}) \neq (\mathbf{p}_0, \mathbf{v}_{\mathrm{c}_0})$, be such that $(\bar{\mathbf{p}}, \bar{\mathbf{v}}_{\mathrm{c}}) \in {}_{\mathbf{B}}\mathcal{I}^{\mathrm{z}}_{\mathrm{rd,uc}}(\mathbf{p}_0, \mathbf{v}_{\mathrm{c}_0})$. Then, for each s, $1 \leq s \leq m$,

$$\|\bar{\mathbf{p}} + \bar{\mathbf{v}}_{\mathrm{tot}}\, t - \mathbf{b}_s\|^2 = \|\mathbf{p}_0 + \mathbf{v}_{\mathrm{tot}}\, t - \mathbf{b}_s\|^2$$

and

$$\mathbf{e}_3^{\mathrm{T}}(\bar{\mathbf{p}} + \bar{\mathbf{v}}_{\mathrm{tot}}\, t - \mathbf{b}_s) = \mathbf{e}_3^{\mathrm{T}}(\mathbf{p}_0 + \mathbf{v}_{\mathrm{tot}}\, t - \mathbf{b}_s)$$

for all $t \in [0, t_f]$, where $\mathbf{v}_{\mathrm{tot}} = \mathbf{v}_0 + \mathbf{v}_{\mathrm{c}_0}$, $\bar{\mathbf{v}}_{\mathrm{tot}} = \mathbf{v}_0 + \bar{\mathbf{v}}_{\mathrm{c}}$ and $\mathbf{v}_0 \in \mathbb{R}^3$ is given by (5.3). This implies that

$$\|\bar{\mathbf{p}} - \mathbf{b}_s\|^2 = \|\mathbf{p}_0 - \mathbf{b}_s\|^2, \tag{7.15}$$

$$\|\bar{\mathbf{v}}_{\mathrm{tot}}\|^2 = \|\mathbf{v}_{\mathrm{tot}}\|^2, \tag{7.16}$$

$$\bar{\mathbf{v}}_{\mathrm{tot}}^{\mathrm{T}}(\bar{\mathbf{p}} - \mathbf{b}_s) = \mathbf{v}_{\mathrm{tot}}^{\mathrm{T}}(\mathbf{p}_0 - \mathbf{b}_s) \tag{7.17}$$

and

$$\mathbf{e}_3^{\mathrm{T}}\bar{\mathbf{p}} = \mathbf{e}_3^{\mathrm{T}}\mathbf{p}_0, \tag{7.18}$$

$$\mathbf{e}_3^{\mathrm{T}}\bar{\mathbf{v}}_{\mathrm{tot}} = \mathbf{e}_3^{\mathrm{T}}\mathbf{v}_{\mathrm{tot}}. \tag{7.19}$$

Let $i, j, k \in \{1, \ldots, m\}$ be such that

$$\mathbf{e}_3^{\mathrm{T}}((\mathbf{b}_i - \mathbf{b}_j) \times (\mathbf{b}_j - \mathbf{b}_k)) \neq 0, \tag{7.20}$$

$$\mathbf{e}_3^{\mathrm{T}}((\mathbf{p}_0 - \mathbf{b}_j) \times (\mathbf{p}_0 - \mathbf{b}_j)) \neq 0. \tag{7.21}$$

Then Eq. (7.15) implies that

$$\left.\begin{aligned} \|\bar{\mathbf{p}} - \mathbf{b}_i\|^2 &= \|\mathbf{p}_0 - \mathbf{b}_i\|^2, \\ \|\bar{\mathbf{p}} - \mathbf{b}_j\|^2 &= \|\mathbf{p}_0 - \mathbf{b}_j\|^2, \\ \|\bar{\mathbf{p}} - \mathbf{b}_k\|^2 &= \|\mathbf{p}_0 - \mathbf{b}_k\|^2. \end{aligned}\right\} \tag{7.22}$$

Taking the differences of $\|\bar{\mathbf{p}} - \mathbf{b}_i\|^2 = \|\mathbf{p}_0 - \mathbf{b}_i\|^2$ and $\|\bar{\mathbf{p}} - \mathbf{b}_j\|^2 = \|\mathbf{p}_0 - \mathbf{b}_j\|^2$ yields

$$(\mathbf{b}_j - \mathbf{b}_i)^{\mathrm{T}}\bar{\mathbf{p}} = (\mathbf{b}_j - \mathbf{b}_i)^{\mathrm{T}}\mathbf{p}_0 \tag{7.23}$$

while taking the differences of $\|\bar{\mathbf{p}} - \mathbf{b}_j\|^2 = \|\mathbf{p}_0 - \mathbf{b}_j\|^2$ and $\|\bar{\mathbf{p}} - \mathbf{b}_k\|^2 = \|\mathbf{p}_0 - \mathbf{b}_k\|^2$ yields

$$(\mathbf{b}_k - \mathbf{b}_j)^{\mathrm{T}}\bar{\mathbf{p}} = (\mathbf{b}_k - \mathbf{b}_j)^{\mathrm{T}}\mathbf{p}_0. \tag{7.24}$$

Eqs. (7.15), (7.23) and (7.24) imply that

$$\begin{bmatrix} (\mathbf{b}_j - \mathbf{b}_i)^{\mathrm{T}} \\ (\mathbf{b}_k - \mathbf{b}_j)^{\mathrm{T}} \\ \mathbf{e}_3^{\mathrm{T}} \end{bmatrix} \bar{\mathbf{p}} = \begin{bmatrix} (\mathbf{b}_j - \mathbf{b}_i)^{\mathrm{T}} \\ (\mathbf{b}_k - \mathbf{b}_j)^{\mathrm{T}} \\ \mathbf{e}_3^{\mathrm{T}} \end{bmatrix} \mathbf{p}_0. \tag{7.25}$$

Please cite this article as: N. Crasta et al., Observability analysis of 3D AUV trimming trajectories in the presence of ocean currents using range and depth measurements, Annual Reviews in Control (2015), http://dx.doi.org/10.1016/j.arcontrol.2015.09.009

Table 5
Observability analysis for zero and nonzero (but constant) yaw rate with multiple range measurements in the weaker sense.

System	Zero yaw rate	Nonzero, constant yaw rate
Known current	$\mathbf{u}^*$- O	$\mathbf{u}^*$- O
Unknown current	$\mathbf{u}^*$- O	$\mathbf{u}^*$- O

$\mathbf{u}^*$-O: $\mathbf{u}^*$-Observable.

Table 6
Observability analysis for zero and nonzero (but constant) yaw rate with multiple range measurements in the Hermann–Krener sense.

System	Zero yaw rate	Nonzero, constant yaw rate
Known current	O	O
Unknown current	O	O

O: Observable.

By assumption the coefficient matrix is invertible and consequently $\bar{\mathbf{p}} = \mathbf{p}_0$. Since $\bar{\mathbf{p}} = \mathbf{p}_0$, Eq. (7.17) with (7.19) yield

$$\begin{bmatrix} (\mathbf{p}_0 - \mathbf{b}_i)^{\mathrm{T}} \\ (\mathbf{p}_0 - \mathbf{b}_j)^{\mathrm{T}} \\ \mathbf{e}_3^{\mathrm{T}} \end{bmatrix} \bar{\mathbf{v}}_{\mathrm{tot}} = \begin{bmatrix} (\mathbf{p}_0 - \mathbf{b}_i)^{\mathrm{T}} \\ (\mathbf{p}_0 - \mathbf{b}_j)^{\mathrm{T}} \\ \mathbf{e}_3^{\mathrm{T}} \end{bmatrix} \mathbf{v}_{\mathrm{tot}}. \tag{7.26}$$

Now the assumption implies that $\bar{\mathbf{v}}_{\mathrm{c}} = \mathbf{v}_{\mathrm{c}_0}$. □

7.2.2. Nonzero, constant yaw rate

Our next result shows that the with at least two distinct transponders, observability can be achieved for nonzero yaw rate in the presence of unknown currents. The proof is similar to that of Proposition 33.

Proposition 35. *Suppose* $m \geq 2$. *Consider* $\|\mathbf{v}_{\mathrm{e}}\|$, $r > 0$, $\gamma \in (-\pi/2, \pi/2)$, *and* $\psi_0, \beta \in [0, 2\pi)$. *Suppose there exist distinct* $k, l \in \{1, \ldots, m\}$ *such that* $\mathbf{e}_3^{\mathrm{T}}(\mathbf{b}_k - \mathbf{b}_l) \neq 0$. *Then, for every* $(\mathbf{p}_0, \mathbf{v}_{\mathrm{c}_0}) \in \mathbb{R}^3 \times \mathbb{R}^3$,

$$_{\mathbf{B}}\mathcal{I}^{\mathrm{nz}}_{\mathrm{r,uc}}(\mathbf{p}_0, \mathbf{v}_{\mathrm{c}_0}) = \{(\mathbf{p}_0, \mathbf{v}_{\mathrm{c}_0})\}. \tag{7.27}$$

Tables 5 and 6 summarizes our findings with multiple range and/or depth as output functions in the weaker and Herman–Krener, sense under suitable assumptions, as shown in the results of this section.

8. Conclusions

This paper provided an analysis of the observability properties of the kinematic model of an autonomous underwater vehicle (AUV) moving in 3D, under the influence of ocean currents, using measurements of its depth and the range to one or more fixed transponders. We exploited the situation where the vehicle undergoes maneuvers commonly known as trimming trajectories, that are naturally obtained when the inputs (thruster rpms and control surface deflections) are held constant. In the case of a single transponder, we showed that for nonzero yaw rate, in the presence of non-zero but known ocean currents, the 3D kinematic model of an AUV undergoing trimming trajectories subject to the condition that the flight-path angle satisfies a current-related constraint is observable. In particular, in the absence of currents the current-related constraint results in a nonzero flight-path angle. However, in the presence of unknown currents, we proved that the model is only weakly observable for nonzero yaw rate. Further, when the latter condition fails, we concluded that the model also fails to be weakly observable. By fusing depth and single range information together, under the assumption that the yaw rate is different from zero, we showed that the 3D kinematic model of an AUV undergoing trimming trajectories subject non-zero unknown currents is observable even when the flight-path angle is zero (vehicle moving in a horizontal plane). These obvious advantages are lost if yaw rate is equal to zero, for in this case the model is only weakly observable. For all situations where the model is weakly observable we gave a complete characterization of the sets of states that are indistinguishable from a given initial state. Finally, we showed that the 3D kinematic model of an AUV undergoing trimming trajectories with multiple (at least two) transponders is observable in all situations if the yaw rate is different from zero. However, zero yaw rate case requires depth information to achieve observability. Future work will aim at exploiting the use of trimming trajectories to estimate the position of an underwater vehicle in 3D using multiple-range localization systems.

References

Arrichiello, F., Antonelli, G., Aguiar, A. P. Pascoal, A. M. (2011). Observability metric for the relative localization of AUVs based on range and depth measurements: theory and experiments. In *Proceedings of IEEE/RSJ international conference on intelligent robots and systems (IROS)* (pp. 3166–3171).

Batista, P., Silvestre, C., & Oliveira, P. (2011). Single range aided navigation and source localization: observability and filter design. *System and Control Letters, 60*(8), 665–673.

Bayat, M., & Aguiar, A. P. (2012). Observability analysis for AUV range-only localization and mapping: measures of unobservability and experimental results. In *Proceedings of IFAC conference on manoeuvring and control of marine craft* (pp. 325–330).

Bayat, M., Crasta, N., Aguiar, A. P., & Pascoal, A. M. (2015). Range-based underwater vehicle localization in the presence of unknown ocean currents: theory and experiments. *IEEE Transactions on Control Systems Technology*.

Crasta, N., Bayat, M., Aguiar, A. P., & Pascoal, A. M. (2013). Observability analysis of the 2D Single-beacon navigation with range-only measurements for two classes of maneuvers. In *Proceedings of IFAC conference on control applications in marine systems* (pp. 227–232).

Crasta, N., Bayat, M., Aguiar, A. P., & Pascoal, A. M. (2014). Observability analysis of 3D AUV trimming trajectories in the presence of ocean currents using single-beacon navigation. In *Proceedings of IFAC world congress* (pp. 4222–4227).

Elgersma, M. R. (1988). *Control of nonlinear systems using partial dynamic inversion (Ph.d. thesis)*. University of Minnesota.

Fossen, T. I. (1994). *Guidance and control of ocean vehicles*. Wiley.

Gadre, A. S., & Stilwell, D. J. (2004). Toward underwater navigation based on range measurements from a single localization. In *Proceedings of IEEE international conference on robotics & automation:* vol. 5 (pp. (4472–4477)).

Gadre, A. S., & Stilwell, D. J. (2005). Underwater navigation in the presence of unknown currents based on range measurements from a single location, vol. 1, (656–661).

Hermann, R., & Krener, A. J. (1977). Nonlinear controllability and observability. *IEEE Transactions on Automatic Control, AC-22*(5), 728–740.

Jouffroy, J., & Reger, J. (2006). An algebraic perspective to single-transponder underwater navigation. In *Proceedings of the IEEE international conference on control applications* (pp. 1789–1794).

Kinsey, J. C., Eustice, R. M., & Whitcomb, L. L. (2006). A survey of underwater vehicle navigation: recent advances and new challenges. In *Proceedings of IFAC conference of manoeuvering and control of marine craft*.

Krener, A. J., & Isidori, A. (1983). Linearization by output injection and nonlinear observers. *System and Control Letters, 3*, 47–52.

Murray, R. M., Li, Z., & Sastry, S. S. (1994). *A mathematical introduction to robotic manipulation*. CRC Press.

Parlangeli, G. Indiveri, G. (2014). Single range observability for cooperative underactuated underwater vehicles. In Proceedings of IFAC world congress pp. 5127–5138. Cape Town, South Africa.

Rugh, W. J. (1996). *Linear systems theory*. London: Prentice Hall Publications.

Sontag, E. D., & Wang, Y. (2008). Uniformly universal inputs. *Analysis and design of nonlinear control systems* (pp. 9–24). Springer.

Naveena Crasta received the B.E. degree in Electrical and Electronics Engineering from the Manipal Institute of Technology, Manipal, in 2000, the M.Tech. degree in Control and Automation from the Indian Institute of Technology Delhi, in 2004, and the Ph.D. in Aerospace Engineering from the Indian Institute of Technology Bombay, in 2009. Currently he is a researcher at the Institute for Systems and Robotics, Instituto Superior Técnico, University of Lisbon, Portugal. His research interests include nonlinear systems theory, dynamics and control of rotational motion, control, navigation, and guidance of autonomous robotic vehicles, nonlinear observers and estimation theory, energy-based control and computational geometry.

Mohammadreza Bayat received his B.Sc. in Electrical Engineering from the Polytechnic University of Tehran (AUT), in 2004, M.Sc. in Automation and Instrumentation Engineering from the Petroleum University of Technology, Tehran, in 2007, and Ph.D. in Computer and Electrical Engineering from Instituto Superior Técnico (IST), University of Lisbon, in 2015. From 2007 to 2015 he was a researcher at Institute for Systems and Robotics (ISR), IST. Currently he is a researcher at Biorobotics Laboratory, Ecole Polytechnique Fédérale de Lausanne. His main research interests include nonlinear robust/adaptive estimation, data reconciliation, nonlinear observers, underwater robot localization and tracking.

Please cite this article as: N. Crasta et al., Observability analysis of 3D AUV trimming trajectories in the presence of ocean currents using range and depth measurements, Annual Reviews in Control (2015), http://dx.doi.org/10.1016/j.arcontrol.2015.09.009

António Pedro Aguiar received the Licenciatura, M.S. and Ph.D. in Electrical and Computer Engineering from Instituto Superior Técnico, University of Lisbon, Portugal in 1994, 1998 and 2002, respectively. Currently, he holds an Associate Professor position with the Department of Electrical and Computer Engineering, Faculty of Engineering, University of Porto. From 2002 to 2005, he was a post-doctoral researcher at the Center for Control, Dynamical-Systems, and Computation at the University of California, Santa Barbara. From 2005 to 2012, he was a senior researcher with ISR/IST, and an invited assistant professor with the Department of Electrical and Computer Engineering, IST. His research interests include modeling, control, navigation, and guidance of autonomous robotic vehicles, nonlinear control, switched and hybrid systems, tracking, path-following, performance limitations, nonlinear observers, the integration of machine vision with feedback control, networked control, and coordinated/cooperative control of multiple autonomous robotic vehicles.

António M. Pascoal received his Ph.D. in Control Science from the University of Minnesota, Minneapolis, MN, USA in 1987. Currently, he is an Associate Professor of Control and Robotics at IST, University of Lisbon, Portugal. He is a member of the Scientific Council of the Institute for Systems and Robotics (ISR), Lisbon. His research interests include dynamical systems theory, robotics, navigation, guidance, and control of autonomous vehicles, and networked control and estimation. He was Elected Chair, IFAC Technical Committee Marine Systems, from 2008–2014. He was IST's responsible scientist for eight EU funded collaborative research projects and several national research projects, all in the area of dynamical systems and ocean/air robotics. He has cooperated extensively with groups in Europe, US, India, and Korea on the development and at sea testing of robotic systems for ocean exploration. His long-term goal is to contribute to the development of advanced technological systems for ocean exploration and exploitation aimed at bridging the gap between science and technology.

Please cite this article as: N. Crasta et al., Observability analysis of 3D AUV trimming trajectories in the presence of ocean currents using range and depth measurements, Annual Reviews in Control (2015), http://dx.doi.org/10.1016/j.arcontrol.2015.09.009